SANDIA REPORT
SAND2009-7228
Unlimited Release
Printed November 2009

LDRD Final Report on "Pumping Up CO_2 and Conversion into Useful Molecules" (LDRD 105932)

Constantine A. Stewart, Diane A. Dickie, and Richard A. Kemp

Prepared by
Sandia National Laboratories
Albuquerque, New Mexico 87185 and Livermore, California 94550

Sandia is a multiprogram laboratory operated by Sandia Corporation,
a Lockheed Martin Company, for the United States Department of Energy's
National Nuclear Security Administration under Contract DE-AC04-94AL85000.

Issued by Sandia National Laboratories, operated for the United States Department of Energy by Sandia Corporation.

Available to DOE and DOE contractors from
U.S. Department of Energy
Office of Scientific and Technical Information
P.O. Box 62
Oak Ridge, TN 37831

Telephone: (865) 576-8401
Facsimile: (865) 576-5728
E-Mail: reports@adonis.osti.gov
Online ordering: http://www.osti.gov/bridge

Available to the public from
U.S. Department of Commerce
National Technical Information Service
5285 Port Royal Rd.
Springfield, VA 22161

Telephone: (800) 553-6847
Facsimile: (703) 605-6900
E-Mail: orders@ntis.fedworld.gov
Online order: http://www.ntis.gov/help/ordermethods.asp?loc=7-4-0#online

SAND2009-7228
Unlimited Release
Printed November 2009

LDRD Final Report on "Pumping Up CO_2 and Conversion into Useful Molecules" (LDRD 105932)

Constantine A. Stewart[†], Diane A. Dickie,[‡] and Richard A. Kemp[†‡]

[†]Ceramic Processing and Inorganic Materials
Sandia National Laboratories
P.O. Box 5800
Albuquerque, New Mexico 87185-MS1349

[‡]Department of Chemistry and Chemical Biology
University of New Mexico
Albuquerque, New Mexico 87131-MSC03 2060

Abstract

Group 12 metal cyclam complexes and their derivatives as well as $(octyl)_2Sn(OMe)_2$ were examined as potential catalysts for the production of dimethyl carbonate (DMC) using CO_2 and methanol. The zinc cyclams will readily take up carbon dioxide and methanol at room temperature and atmospheric pressure to give the metal methyl carbonate. The tin exhibited an improvement in DMC yields.

Studies involving the reaction of bis-phosphino- and (phosphino)(silyl)-amido group 2 and 12 complexes with CO_2 and CS_2 were performed. Notable results include formation of phosphino-substituted isocyanates, fixation of three moles of CO_2 in an unprecedented $[N(CO_2)_3]^{3-}$ anion, and rapid splitting of CS_2 by main group elements under extremely mild conditions.

Similar investigations of divalent group 14 silyl amides led to room temperature splitting of CO_2 into CO and metal oxide clusters, and the formation of isocyanates and carbodiimides.

ACKNOWLEDGMENTS

We would like to thank Dr. Eric Coker (1815) for the templated carbon supports and Marie Parkes (UNM) for DFT calculations and helpful discussion. Drs. Ana Felix, Brian Boro, Yongjun Tang (all UNM) performed some of the experimental work described herein. Partial funding was provided by the National Science Foundation and the Natural Science and Engineering Research Council of Canada (Post-Doctoral fellowship for D. Dickie).

CONTENTS

FIGURES

SCHEMES

TABLES

NOMENCLATURE

[16]aneN_4	1,5,9,13-tetraazacyclohexadecane
[14]aneN_4	1,4,8,11-tetraazacyclotetradecane
B3LYP/LACVP	Density functional theory - Becke, three-parameter, Lee-Yang-Parr
Ad	adamantyl
cy	cyclohexyl
cyclam	1,4,8,11-tetraazacyclotetradecane
cyclam-2MP	1-pyridin-2-ylmethyl-1,4,8,11-tetraazacyclotetradecane
cyclam-3MP	1-pyridin-3-ylmethyl-1,4,8,11-tetra azacyclotetradecane
DMAP	4-dimethylaminopyridine
DMC	dimethyl carbonate
GC-MS	gas chromatography – mass spectrum
Group 2	elements in the 2nd row of the periodic table (Mg, Ca, Sr)
Group 12	elements in the 12th row of the periodic table (Zn, Cd, Hg)
Group 14	elements in the 14th row of the periodic table (C, Si, Ge, Sn, Pb)
i-Pr	isopropyl
IR	infrared
Me	methyl
NMR	nuclear magnetic resonance
py	pyridine
ppm	parts per million
TEG	thermally expanded graphite
THF	tetrahydrofuran
tmdacp	2,2,5,5-**t**etra**m**ethyl-2,5-**d**isila-1-**a**za-**c**yclo**p**entane
μ	denotes the number of bridging bonds in an atom
η	hapticity (from the Greek -ηαππειυ haptien to fasten) denotes number of atoms attached to the metal

1 INTRODUCTION

Currently there may be no more critical issue facing us over the next several decades than CO_2 production and its effect on global warming. Conveniently-obtained oil is approaching the end of an era and the availability and cost of transportation fuels continues to increase. It is now clear that the potential magnitude of these problems can have an impact national security. It is also clear that the problems are complex and require the attention of the nation's research establishment. It is assumed that carbon dioxide capture and sequestration can be carried out on a large scale, *e.g.*, at coal-fired power plants, yet there are no large-scale demonstrations that prove this can be accomplished at acceptable costs. The prospect of geological disposal of carbon dioxide is an inelegant solution and does not preclude the dependence on fossil fuels. A more desirable route would be to recycle CO_2 as a C1 source into high value chemical synthons such isocyanates or carbodiimides or a fuel product (i.e. dimethyl carbonate which is also a valuable chemical intermediate). This is not a trivial problem because carbon dioxide is already an energetically "depleted" molecule.

In this project we studied a variety of routes that combined CO_2 with methanol to make dimethyl carbonate, and with metal amides to give isocyanates and carbodiimides. However, more work will be needed to make these processes catalytic. In addition we also investigated the potential for capturing carbon dioxide and sequestering it by chemically binding it with a variety metal amides. Finally we studied a number of metal complexes with not only carbon dioxide but also other carbon dichalcogenides (COS and CS_2) with the goal of understanding how to activate CO_2. These fundamental studies led to surprising and unexpected results regarding reactivity and bonding modes of carbon dioxide and its analogs. These results can potentially lead us into new areas and approaches for research towards carbon capturing and sequestration.

2 RESULTS AND DISCUSSION

2.1 Dialkyl Dimethoxy Tin Complexes as Potential Catalysts for the Production of Dimethyl Carbonate

Dialkyl dimethoxy tin compounds have been found to convert carbon dioxide and methanol to dimethyl carbonate (DMC).[1-4] This work has been reported by a number of groups over the last dozen years. The two major drawbacks with these tin based catalysts are their vulnerability to hydrolysis and the extreme conditions (~ 4350 psi at 180 °C for 24 hrs) required to convert CO_2 and methanol to DMC, see Scheme 2.1.1.[5]

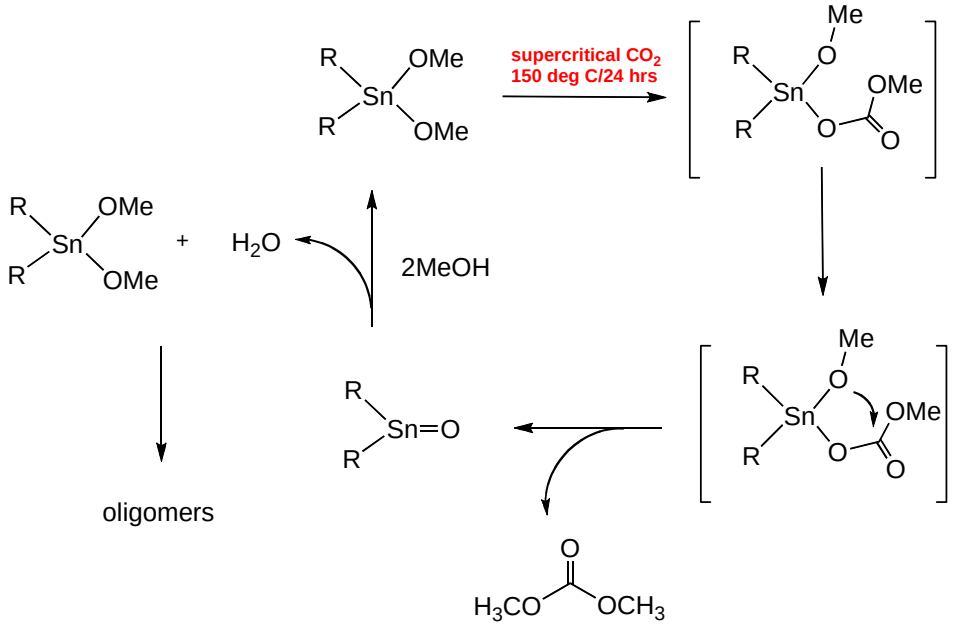

Scheme 2.1.1 Mechanism for the conversion of CO_2 and methanol using dialkyl dimethoxy tin catalyst.

The alkyl groups of choice for this dialkyl dimethoxy tin catalyst are *n*-butyl. While other groups such as branched alkyls (*t*-butyl) and even aryls (phenyl) have been investigated, the di-*n*-butyl dimethoxy tin compound has shown the best results for producing DMC. In an effort to make this type of tin catalyst more stable towards hydrolysis, without affecting its productivity, we decided to substitute the butyl groups for octyl groups. It is known that compounds containing long chain hydrocarbons are hydrophobic and potentially more stable towards water. This should make the di-*n*-octyl dimethoxy tin molecule less susceptible to hydrolysis and given that the octyl groups are still linear not degrade its performance as a DMC catalyst.

Preliminary work for this part of the project involved preparing a reactor system that could handle very high pressures of carbon dioxide at high temperatures. The optimal reactor for this work was a Parr reactor with a 100 cc bowl fitted with a 3,000 psi

pressure relief disc. Conventional pressure relief valves could not be used for this work due to the unsuitability of the o-rings in the sealing sections with such high pressures of CO_2. The o-rings tend to take up CO_2 at very high pressures and once the pressure is relieved the rapid out-gassing of the carbon dioxide causes degradation of the rubber. To test the system, a sample of (*n*-octyl)$_2$Sn(OMe)$_2$ was prepared. The tin catalyst was charged to the reactor with methanol under argon and heated to ~ 155 °C. The reactor was then pressurized with carbon dioxide to 2,100 psi using a high-pressure Whitey compressor. The reaction was allowed to proceed at that temperature for 18 hours. At the end of the reaction the reactor was vented and the contents removed. There was a white precipitate (hydrolyzed catalyst – tin alkyl oxide oligomers) and a pale amber solution. The solution contained methanol and dimethyl carbonate (~ 0.13% DMC over 18 hours). This initial yield compares favorably with results reported by Ballivet-Tkatchenko and coworkers.[6] They reported DMC yields (DMC/[$Bu_2Sn(OMe)_2$], mol/(mol/L)) as a function of reaction time and CO_2 pressure at 114 °C. For the catalyst $Bu_2Sn(OMe)_2$ run at 114 °C at 2,930 psi after 24 hrs they obtained 0.03 mol of DMC/[mol Sn/L] at a mmol ratio of 225/556/1.50 for CH_3OH/CO_2/Sn. From our initial results for (*n*-octyl)$_2$Sn(OMe)$_2$ we estimate a value of 2.5 mol of DMC/[mol Sn/L] run at 150 °C at a pressure of 2,100 psi CO_2 for ~ 18 hrs. The molar ratio of CH_3OH/Sn was equal to 750/4. The amount of carbon dioxide in the reaction could not be determined precisely at this point because of the uncertainty in measuring the volume of the head space.

Our initial results with (*n*-octyl)$_2$Sn(OMe)$_2$ catalysts indeed look very promising, but it must be verified with multiple runs and under other conditions. However, the problem still remains that even with the more hydrophobic di-octyl groups on the tin, this catalyst is still susceptible to hydrolysis and therein is the problem with using these types of tin reagents as catalysts for the production of DMC where water is the by-product. There is no simple way of getting around the water issue when making dimethyl carbonate from methanol and carbon dioxide. What is needed is a catalyst system that operates under milder conditions and is stable to water. The next section addresses these two issues of less extreme conditions for the reaction of methanol and CO_2, and water stability.

2.2 Metal Cyclam Complexes as Potential Catalysts for the Production of Dimethyl Carbonate

Our interest in metal 1,4,8,11-tetraazacyclotetradecanes (cyclams) is based on their propensity to take up CO_2 at ambient temperatures and pressure. This facile uptake of CO_2 to give a carbonato metal complex was first reported by Kato and Ito for zinc cyclams.[7,8] The cavity size of the tetraazacycloalkanes is important in order for the metal to give the carbonato complex.[9] According to Kato and Ito, zinc takes up CO_2 most readily, if it is not allowed to form the more stable tetrahedral geometry. Therefore neither the linear tetraamines nor the larger 1,5,9,13-tetraazacyclohexadecane ([16]aneN_4) will produce the methyl carbonate zinc complexes. In addition, the substituents on the nitrogen atoms, in this case methyl groups, determine the not only the ring configuration but also inter-molecular coordination between the zinc cyclams (Scheme 2.2.1).

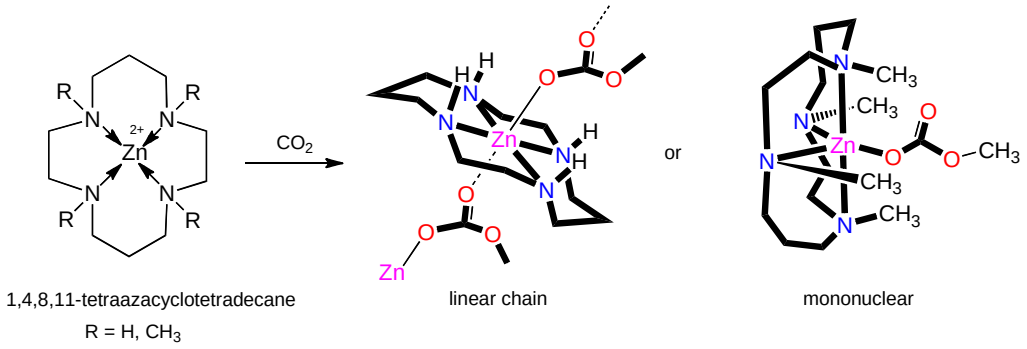

Scheme 2.2.1 Linear chain versus mononuclear zinc cyclam complexes based on nitrogen substitution.

When the cyclam nitrogen atoms have hydrogen attached, a chain network of zinc atoms connected to carbonato groups occurs. On the other hand, when the nitrogen atoms contain methyl groups a monomeric zinc complex is formed and the local coordination around the zinc center adopts a trigonal-bipyramid configuration.

As can be seen from this scheme, the zinc methyl carbonate complex is poised to produce dimethyl carbonate with the insertion of another molecule of methanol (Scheme 2.2.2). The potential advantage to the zinc cyclam systems over the dialkyl dimethoxy tin catalysts is that they readily take up CO_2 at room temperature and pressure in the presence of methanol to make the metal methyl carbonate complex. This methyl carbonate species is essentially two-thirds of the way to the formation of dimethyl carbonate. Additionally, these metal methyl carbonates are stable to water, which the dialkyl dimethoxy tin catalysts for DMC production are not.

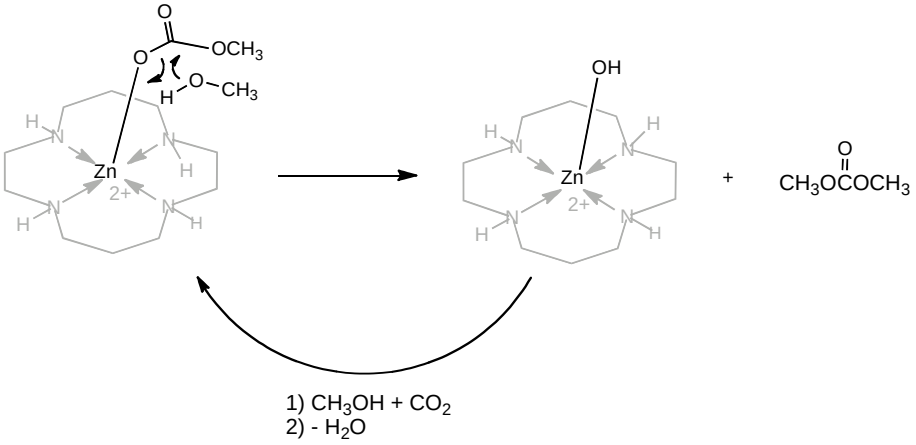

Scheme 2.2.2 Proposed catalytic route to the formation of DMC using a zinc cyclam complex.

Other transition metal cyclams (Ni) will also take up CO_2, but less readily than zinc; therefore we concentrated our efforts on exploring the chemistry of these Group 12 metals (Zn, Cd and Hg) as possible catalysts for the formation of dimethylcarbonate.

2.2.1 Attempts to Eliminate Dimethyl Carbonate from the Metal Methyl Carbonate Complex

Ito reported that these zinc cyclams not only take up CO_2 at room temperature and atmospheric pressure, but that this process is reversible.[7-9] Our goal was to determine if under the right conditions another molecule of methanol could be added to the metal methyl carbonate complex to eliminate DMC. Since it is known that these complexes will release CO_2 at elevated temperatures, the initial approach was to try somewhat mild conditions with $Zn[14]aneN_4[ClO_4]_2$ in the presence of methanol and CO_2 at roughly the ratio of 2.5:1 and moderate pressures of carbon dioxide (100 psig) at room temperature. Reactions at these parameters or even at higher temperatures and pressures did not produce any evidence of DMC.

The next strategy was to investigate various forcing conditions such as high temperatures and very high pressures of carbon dioxide. This approach involved the use of very high pressures of carbon dioxide at room temperature with zinc cyclam and methanol (Scheme 2.2.3). Gas chromatography-mass spectra (GC-MS) analysis of the reaction solution did not reveal the presence of dimethyl carbonate or any other products. For the second attempt a higher temperature was employed (80 °C) with the same reaction time. Again, the analysis of the reaction mixture showed no evidence of dimethyl carbonate or any other products. Only methanol and dissolved CO_2 were evident in the GC-MS. The last attempt was to use slightly higher temperatures and pressure (100 °C at 2,300 psi) and the addition of methoxide as a cocatalyst.[10] There again we saw nothing but starting materials in the GC-MS.

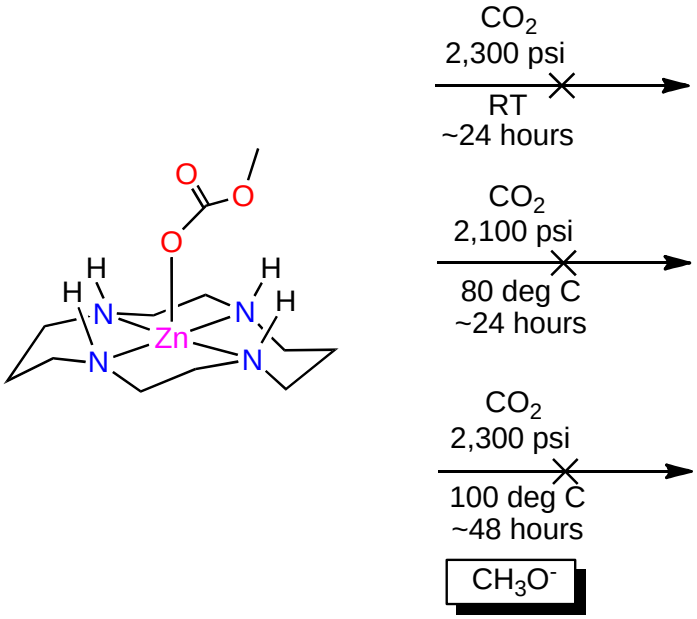

Scheme 2.2.3 Attempts to form DMC using zinc cyclam, CO_2 and methanol.

2.2.2 *Modification of the Cyclam Complex Via the Addition of Functionalized Arms*

In the absence of any activity for the parent Zn[14]aneN_4[ClO_4]$_2$ towards the elimination of dimethyl carbonate under mild to extreme reaction conditions the next alternative was to modify the macrocycle by attachment of a Lewis basic ligand group (Figure 2.2.1). This approach is based on two possible paths towards the incorporation of the second molecule of methanol and subsequent elimination of DMC. The first is the base-assisted deprotonation of the incoming methanol to make the oxygen more nucleophilic towards the carbonyl carbon. The second scenario is the backside attack of the basic ligand at the metal site leading to a bond polarization change in the metal methyl carbonate. This change in bond polarity and strength could be enough to assist in the addition of a second molecule of methanol. The potential downside of attaching a Lewis base group is that the base could strongly complex to the metal center and thus prevent the formation of the methyl carbonate.

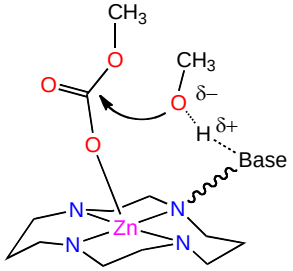

Intra-sphere base assisted deprotonation of incoming methanol

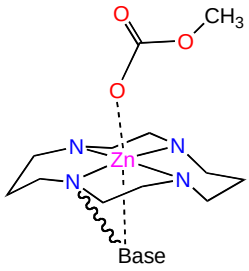

backside "attack" of the Lewis Base ligand at the metal

Figure 2.2.1 Modification of the cyclam macrocycle by the attachment of a Lewis base arm.

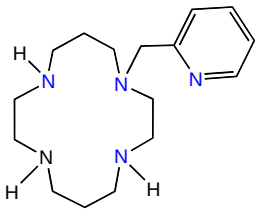

1-pyridin-2-ylmethyl-1,4,8,11-tetraazacyclotetradecane

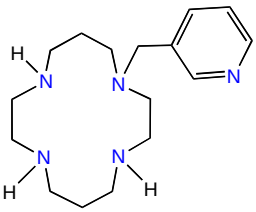

1-pyridin-3-ylmethyl-1,4,8,11-tetraazacyclotetradecane

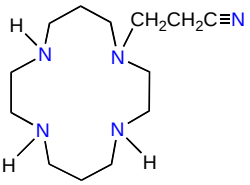

3-(1,4,8,11-tetraazacyclo tetradecan-1-yl)propionitrile

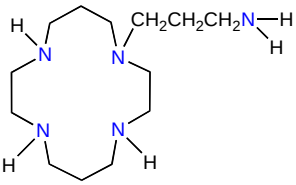

1-(3-aminopropyl)-1,4,8,11-tetraazacyclotetradecane

Figure 2.2.2 Substituted cyclams with Lewis basic groups.

Possible substituted cyclams with Lewis basic groups attached to one of the nitrogens in the macrocycle are shown in Figure 2.2.2. These pendant nitrogen ligands range from strong bases (-NH_2) to weak (CN). The 1-pyridin-2-ylmethyl-1,4,8,11-tetraazacyclotetradecane (cyclam-2MP) and 1-pyridin-3-ylmethyl-1,4,8,11-tetraazacyclotetradecane (cyclam-3MP) complexes were synthesized first by the method of Guilard.[11] These substituted cyclams were isolated as oils but over time crystallized which allowed for the determination of their structures by X-ray crystallography, which are shown in Figure 2.2.3.

Cyclam-2MP
1-pyridin-2-ylmethyl-1,4,8,11-tetra azacyclotetradecane

Cyclam-3MP
1-pyridin-3-ylmethyl-1,4,8,11-tetra azacyclotetradecane

Figure 2.2.3 X-ray structures of cyclam-2MP and cyclam-3MP. For clarity, only N-H hydrogen atoms are shown.

The Zn-cyclam-2MP, Cd-cyclam-2MP and Zn-3MP complexes were prepared from the metal perchlorate salts. The Zn-cyclam-2MP and the Cd-cyclam-2MP were crystallized and their molecular structures determined by single crystal X-ray diffraction (Figure 2.2.4). Due to the atomic radii differences between zinc and cadmium (Zn (atomic radius) = 1.35 Å; Cd (atomic radius) = 1.55 Å) there is a noticeable difference in how far out of the plane the cadmium is versus the zinc. Interestingly enough, these two metal cyclams crystallize as mirror images of one another and both adopt the trans-1 configuration.

Cd-Cyclam-2MP Zn-Cyclam-3MP

Figure 2.2.4 X-ray structures of Cd-cyclam-2MP and Zn-cyclam-3MP. For clarity, only N-H hydrogen atoms are shown, and the ClO_4^- anions have been omitted.

The Zn-cyclam-3MP complex seems to have formed, but the resulting microcrystalline solid that was isolated from the reaction mixture could not be coaxed back into solution. This insolubility suggests that the complex could be a linear polymer of zinc cyclam units bridged by the pyridinyl groups. This would be similar to the solid state structure of the parent Zn-cyclam-methylcarbonate species described by Kato, refer to Scheme 2.2.1.[7]

The Zn-cyclam-2MP complex was reacted with carbon dioxide in the presence of methanol under a variety of conditions from mild to extreme (room temperature at 1 atmosphere of pressure of CO_2 to 170 °C at > 2000 psi of CO_2). The pyridinyl nitrogen was so strongly bound to the zinc that it was not possible to even form the methyl carbonate complex (based on IR spectroscopy). Given that the surface of the cadmium atom is more exposed in the Cd-cyclam-2MP complex, it was also subjected to CO_2 in the presence of methanol; however, no formation of the methyl carbonate was detected. Again this is most probably due to the fact that the pyridinyl nitrogen is strongly coordinated to the metal center.

In an effort to continue the exploration of the concept of using a Lewis basic ligand as an assisting group to escort the dimethyl carbonate off of the metal center, one last substituted cyclam was prepared - 1-propionitrile-1,4,8,11-tetraazacyclotetradecane (cyclam-1PN) and structurally characterized, see Figure 2.2.5.

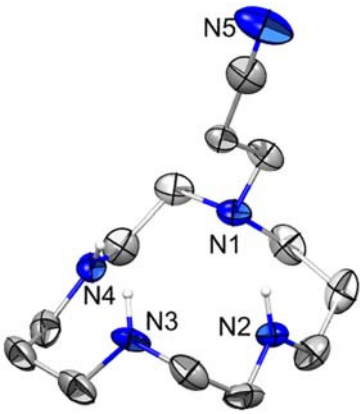

Figure 2.2.5 X-ray structure of 1-propionitrile-1,4,8,11-tetraazacyclotetradecane cyclam-1PN. For clarity only the N-H hydrogen atoms are shown.

This substituted cyclam was prepared following the preparation described by Tfouni and coworkers.[12] Surprisingly, when the zinc cyclam-1PN complex was reacted with CO_2 in the presence of methanol/triethylamine, the propionitrile arm was converted to an ester (Scheme 2.2.4).

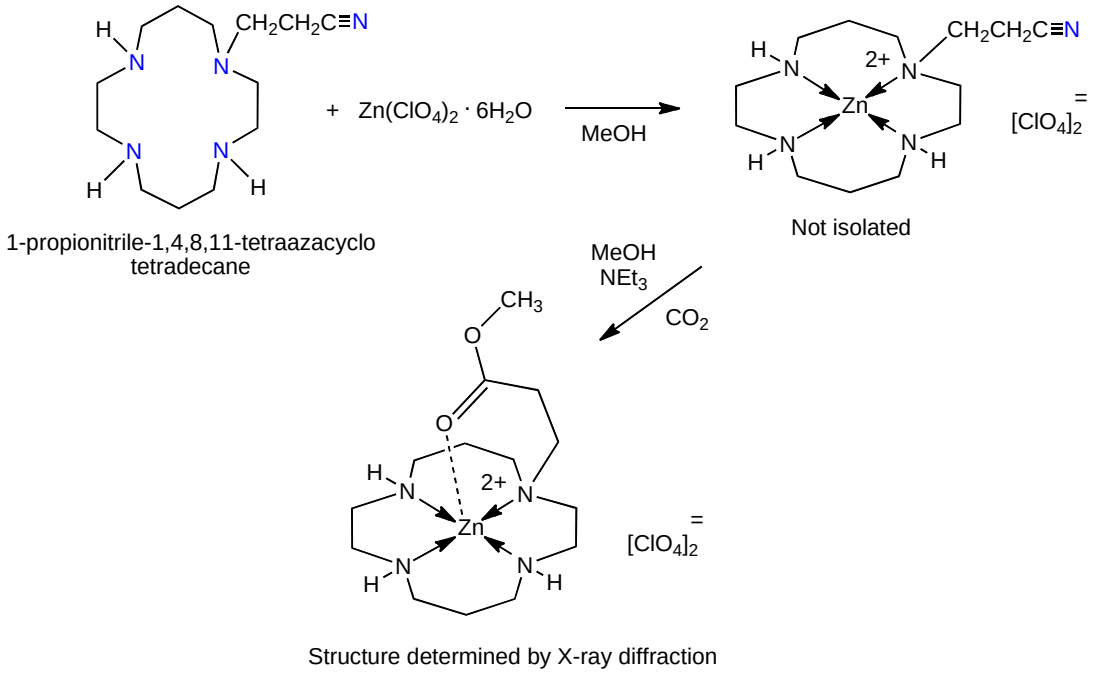

Scheme 2.2.4 Synthetic route to the methylpropylester zinc cyclam.

The structure of this ester substituted cyclam zinc complex was determined by X-ray crystallography (Figure 2.2.6). This reaction is rather unusual in that a nitrile is directly converted to an ester and must have occurred by first hydrolyzing the nitrile to the amide (recall the zinc perchlorate is hydrated with six molecules of water) followed by the alcoholysis of the amide to the ester. This is similar to the Pinner reaction.[13,14] It would be interesting to see if zinc cyclams can directly convert nitriles to esters.

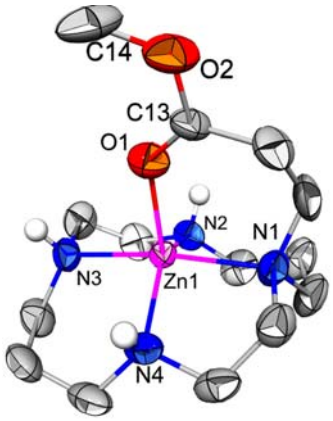

Figure 2.2.6 X-ray structure of methylpropylester zinc cyclam. For clarity, only N-H hydrogen atoms are shown, and the ClO_4^- anions have been omitted.

2.2.3 Summary of Work on Metal Cyclams

These parent metal (zinc) cyclams showed great promise as potential catalysts for the production of dimethyl carbonate from methanol and water. The zinc cyclam will take up carbon dioxide from the air in the presence of methanol to give the zinc methyl carbonate. This process is reversible. However, conditions in which to get the second molecule of methanol into the reaction sphere at the zinc center in order to give dimethyl carbonate could not be found. Various modifications to the cyclam ring through the addition of arms containing pendant nitrogen atoms in which to help assist in either the deprotonation of the second molecule of methanol and increase the nucleophilicity of the methoxide, or change the electronics at the metal center were unsuccessful. A number of new zinc and cadmium complexes using the 1-pyridin-2-ylmethyl-1,4,8,11-tetraazacyclotetradecane cyclam were prepared and the structures determined by X-ray crystallography. Two manuscripts are in preparation describing this work.

In addition, a new zinc 1-propionitrile-1,4,8,11-tetraazacyclotetradecane cyclam complex was prepared and under very mild conditions converted the propionitrile group to an ester. This reaction requires further investigation due to its novelty.

The zinc cyclams are clearly very interesting systems in that they readily take up CO_2 in methanol to give a fragment that is already two thirds of the way to DMC. As an added bonus these complexes are very stable to water. There are other ways to modify the cyclam ring system that might make the zinc center more amenable to accepting the second molecule of methanol and liberating DMC. This could be accomplished by other appendages, “helper” ligands that would assist in the mechanism of bringing in a second molecule of methanol. Alternatively the use of groups attached directly to the nitrogens in the cyclam ring could change the electronics of the zinc making it catalytically active towards the production of DMC.

2.3 Other Systems Investigated for the Potential of Making Dimethyl Carbonate

The literature was followed on an ongoing basis to monitor the activity of other groups working on finding uses for carbon dioxide during the course of this project. One of the systems that appeared to show promise as reported by Xiao and coworkers was a nano catalyst system of copper-nickel supported on graphite that produced dimethyl carbonate in the presence of CO_2.[15,16] They claimed that a nano-(Cu-Ni) on thermally expanded graphite (TEG) catalyst produced DMC at 105 °C with a pressure of 200 psi of CO_2 giving a 9% yield of DMC and a 10% conversion of CH_3OH using a flow through reactor system at a mole ratio of 2:1 CH_3OH:CO_2. We decided to investigate this system and others similar to it.

Three nano-(copper-nickel) on carbon systems were prepared towards the end of this project. One consisted of nano-(Cu-Ni) on a zeolite templated carbon support (from E. N. Coker – Dept. 1815). The second system was nano-(Cu-Ni) on graphite (Norit A Supra) and the third system was very similar to that used in the report by Xiao and coworkers which was nano-(Cu-Ni) on thermally expanded graphite (TEG). The preparation for these systems can be found in the experimental section. All three systems were analyzed by powder X-ray diffraction and found to exhibit similar peaks in the spectra to those published by Xiao. This result confirmed that we had made nano-(Cu-Ni) particles on carbon. Our next step was to evaluate these graphite-supported metal systems as potential DMC catalysts using carbon dioxide and methanol. Unfortunately the Zeton Altamira flow through reactor system was down due to a pressure system upgrade during the last part of this project so all three systems were investigated under bulk conditions. The potential catalysts were slurried in methanol and the reactor pressurized with carbon dioxide to give an estimated final pressure of ~ 200 psi at ~ 105 °C. The systems were run under similar conditions (i.e. CO_2 pressure and temperature as well as mole ratio of MeOH:CO_2) as those reported by Xiao. However, we were unable to detect any DMC in the resulting reaction mixture. This could be due to the fact that our three systems were run under bulk conditions rather than in the gas phase. It would still be beneficial to evaluate these potential catalysts using the flow through reactor system when it is back in operation. There are numerous ways in which to modify a heterogeneous catalyst system such as this to optimize activity, yield, selectivity and lifetime. If the results from the literature report on these catalysts are accurate and reproducible the nano-(Cu-Ni) on TEG certainly requires more study.

2.4 Investigation of Model Systems for the Activation of CO_2

It is well known that carbon dioxide will insert into transition metal-nitrogen bonds to give metal carbamates. Recently we[17-19] and others[20-23] have extended these investigations to divalent amides and silyl amides of group 2, 12 and 14 in an effort to better understand the reaction chemistry and potential routes to isocyanates and carbodiimides. Sita *et al.* have reported the reaction of CO_2 with bis[*N,N'*,-bis (trimethylsilyl)amino]tin(II), $[(Me_3Si)_2N]_2Sn$ and bis[*N,N'*,-bis(trimethylsilyl)amino] germanium(II), $[(Me_3Si)_2N]_2Ge$ to afford the bis-alkoxide complexes $[Sn(OSiMe_3)_2]_2$ and $[Ge(OSiMe_3)_2]_2$ respectively in high yields (Scheme 2.4.1).[22] In addition to the production of the bis-alkoxide metal complexes, Me_3SiNCO (trimethylsilyl isocyanate) and $Me_3Si\text{-}N{=}C{=}N\text{-}SiMe_3$ (1,3-bis(trimethylsilyl) carbodiimide) were produced in good yields.

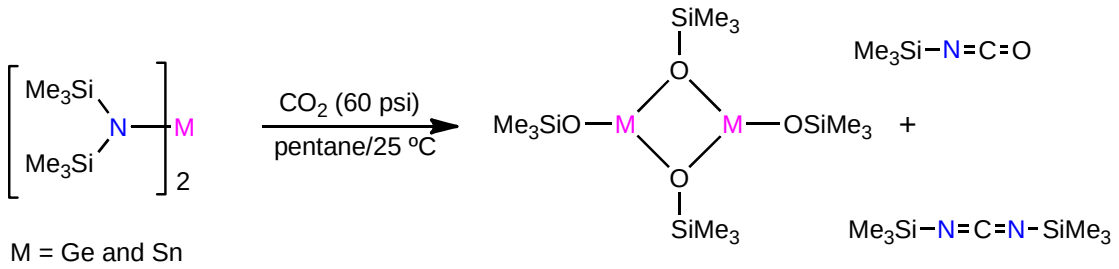

Scheme 2.4.1 The reactions of group 14 metal silyl amides with CO_2.

Unexpectedly, the treatment of $[(Me_3Si)_2N]_2Sn$ with CS_2 gave no reaction even at elevated temperatures.[21] It is somewhat puzzling that $[(Me_3Si)_2N]_2Sn$ will react readily with CO_2 but not CS_2 even under extreme conditions. This prompted us to investigate other reactions of carbon dichalcogenides (CE_2, E = O, S) with a series of silyl amides in the hopes of understanding the chemistry of these small molecules with the eventual understanding of how to activate CO_2 and open up chemical routes in which to convert this molecule to useful products including isocyanates and carbodiimides.

Our objective was to de-convolute the steric and electronic factors between divalent metal silyl amides and CE_2. Several questions came to mind as we formulated our approach to these systems. Was the inability of CS_2 to react with $[(Me_3Si)_2N]_2Sn$ caused purely by a steric effect, or were there perhaps electronic factors involved? The steric component preventing reactivity could be due to a combination of the sterically-demanding bis(trimethylsilyl)amide ligand and a larger sulfur atom (covalent radius $_{sulfur}$ = 1.05 Å vs. covalent radius $_{oxygen}$ = 0.66 Å). As well, we had questions as to where carbonyl sulfide (OCS) would reside in the order of reactivity. OCS has a dipole moment and a central carbon with an electron density value presumably somewhere between CO_2 and CS_2, and so OCS might be expected to exhibit reactivity intermediate to CO_2 and CS_2. Furthermore, what would be the effect of changing from group 14 metals to more electropositive group 2 or 12 metals? Could the silyl group on the ligand be varied to control or increase the selectivity of isocyanate and/or carbodiimide elimination? The results of our investigations into these questions are described in the following sections.

2.4.1 Reactivity of Tin(II) Silyl Amide Complexes with CO_2, OCS and CS_2

We speculated that we might disentangle the effects of sterics while maintaining comparable electronics in the tin silyl amides by using a less sterically crowded ligand that is similar in nature to -$N(SiMe_3)_2$. We postulated that $[(Me_3Si)_2N]_2Sn$ could be compared to bis(2,2,5,5-**t**etra**m**ethyl-2,5-**d**isila-1-**a**za-**c**yclo**p**ent-1-yl)tin ($[tmdacp]_2Sn$) with minimal differences in electronics at the centers of interest. The tin amide $[tmdacp]_2Sn$ is simply a "tied-back" version of $[(Me_3Si)_2N]_2Sn$, and can be prepared from the cyclic 2,2,5,5-**t**etra**m**ethyl-2,5-**d**isila-1-**a**za-**c**yclo**p**entane (tmdacp) ligand (Figure 2.4.1).

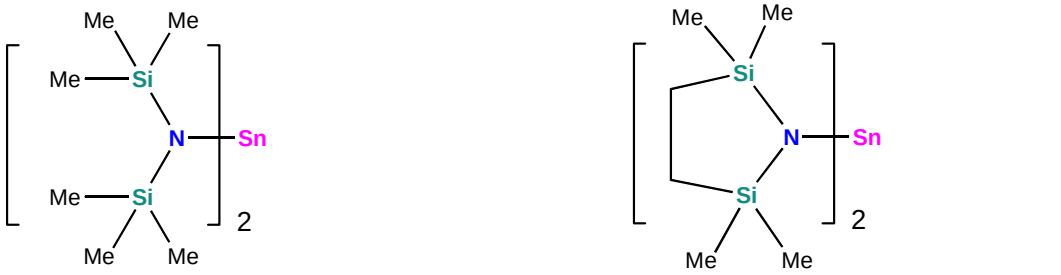

Bis[*N,N'*-bis(trimethylsilyl)amino]tin(II)
$[(Me_3Si)_2N]_2Sn$

Bis(2,2,5,5-tetramethyl-1-aza-2,5-disilacyclopent-1-yl)tin(II)
$(tmdacp)_2Sn$

Figure 2.4.1 Structures of $[(Me_3Si)_2N]_2Sn$ and $(tmdacp)_2Sn$.

DFT calculations were performed to see how these two tin amides compare in terms of tin-nitrogen bond lengths and angles, and charges on the tin, nitrogen and silicon atoms. The results are summarized in Table 2.4.1. In addition, the cone angles for the amide groups have been calculated to give a comparison between the two molecules. As expected the "tied back" silyl amide has a more acute cone angle than that of the bis-trimethyl silyl amide (123° versus 144° respectively). Overall, our goal was to establish the reactivity patterns for these carbon dichalcogenides towards subvalent group 14 complexes containing silyl amides.

Our first objective was to fill in the blank between CO_2 and CS_2 by reacting OCS with $[(Me_3Si)_2N]_2Sn$, see Scheme 2.4.2 below. $[(Me_3Si)_2N]_2Sn$ reacted readily with OCS to give $Sn_4(\mu_4\text{-}O)(\mu_2\text{-}OSiMe_3)_5(\eta^1\text{-}N{=}C{=}S)$.

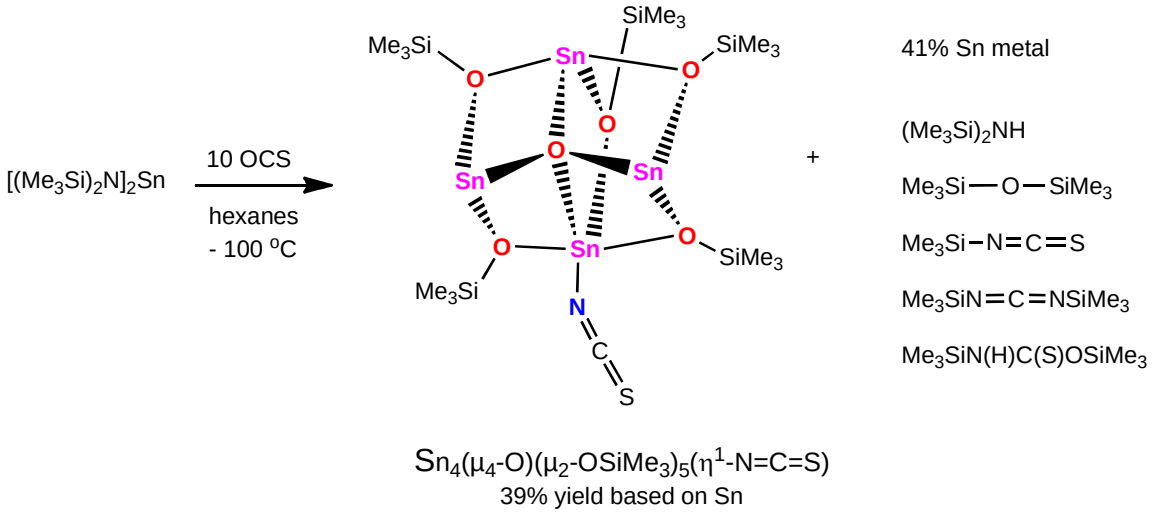

Scheme 2.4.2 Reaction of $[(Me_3Si)_2N]_2Sn$ with excess carbonyl sulfide.

The X-ray structure of $Sn_4(\mu_4\text{-}O)(\mu_2\text{-}OSiMe_3)_5(\eta^1\text{-}N{=}C{=}S)$, shown below in Figure 2.4.2, consists of three different Sn^{II} atoms. Sn(2) and Sn(4) are 3-coordinate, while Sn(3) is 4-coordinate and Sn(1) is 5-coordinate.

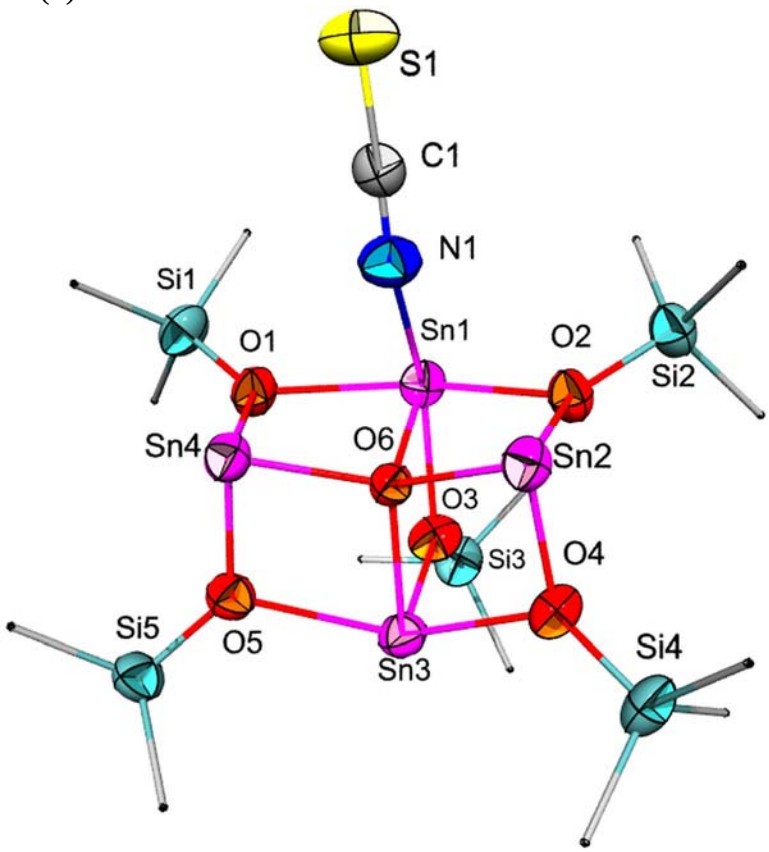

Figure 2.4.2 X-ray structure of $Sn_4(\mu_4\text{-}O)(\mu_2\text{-}OSiMe_3)_5(\eta^1\text{-}N{=}C{=}S)$. For clarity, hydrogen atoms are not shown.

Upon closer inspection of the unit cell of $Sn_4(\mu_4\text{-}O)(\mu_2\text{-}OSiMe_3)_5(\eta^1\text{-}N{=}C{=}S)$ it can be seen that the terminal sulfur atoms are interacting with the three of the tin atoms in a neighbouring molecule (Figure 2.4.3).

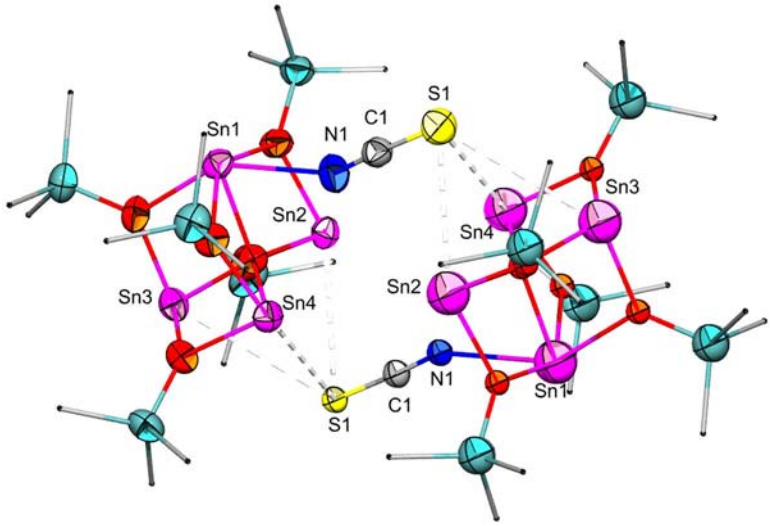

Figure 2.4.3 X-ray structure of $Sn_4(\mu_4\text{-}O)(\mu_2\text{-}OSiMe_3)_5(\eta^1\text{-}N{=}C{=}S)$ with close interactions of neighbouring molecule. For clarity, hydrogen atoms are not shown.

The next series of reactions involved $[tmdacp]_2Sn$ with CO_2, OCS and CS_2. This tin(II) silyl amide reacts readily with CO_2, as expected due to the smaller cone angle of the amide ligands, to give another $(\mu_4\text{-}O)Sn_4$ cluster - $Sn_4(\mu_4\text{-}O)(\mu_2\text{-}O_2C[tmdacp]_4)(\mu_2\text{-}N{=}C{=}O)_2$, see the reaction Scheme 2.4.3 below. What was unexpected was the presence of CO in the headspace of the reaction. This is suggestive of the splitting of CO_2 into oxygen and CO.

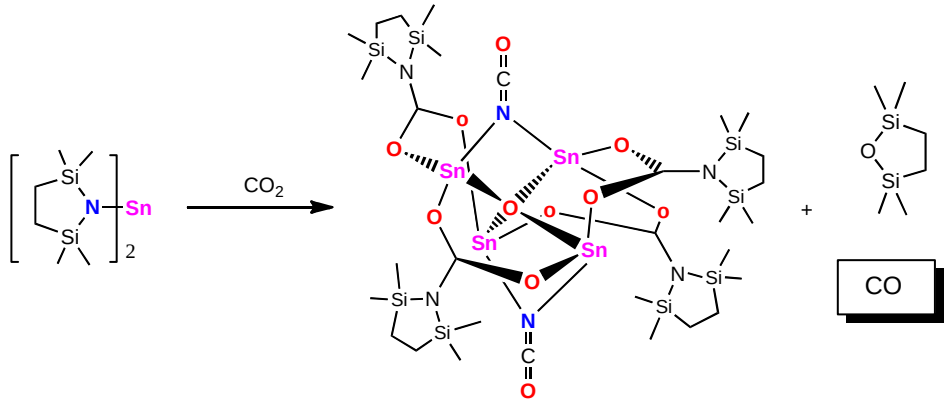

$Sn_4(\mu_4\text{-}O)(\mu_2\text{-}O_2C[tmdacp]_4)(\mu_2\text{-}N{=}C{=}O)_2$
50% yield based on tin

Scheme 2.4.3 Reaction of $(tmdacp)_2Sn$ with CO_2.

The next reaction in this series was $[tmdacp]_2Sn$ with OCS. This reaction proceeded very rapidly to give an intractable rust brown solid that was insoluble in all solvents. The IR spectrum suggests the presence of -N=C=S. The elemental analysis of the solid showed it to be made up of mostly nitrogen, carbon, sulfur and tin. From the elemental analysis

the polymer composition appears to be $Sn_3(NCS)_4(C_6H_{16}OSi_2)_{0.5}$; ($C_6H_{16}OSi_2$) = 2,2,5,5-tetramethyl-2,5-disila-tetrahydrofuran.

The final reaction in this series was $[tmdacp]_2Sn$ with CS_2. This reaction was probably the most straightforward, but also the most odd of the lot. This tin(II) silyl amide reacts very rapidly with excess carbon disulfide to give an instantaneous dark green solution. The product is isolated as a dark green crystalline material in almost quantitative yield. The reaction is shown below in Scheme 2.4.4.

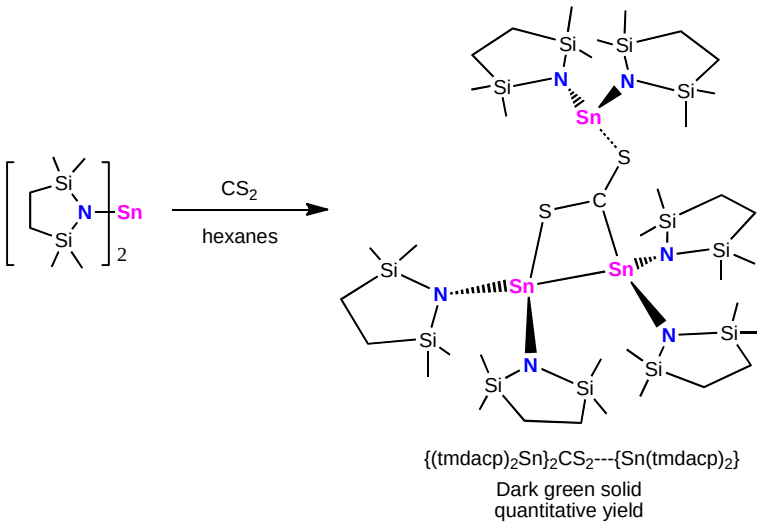

Scheme 2.4.4 Reaction of $(tmdacp)_2Sn$ with CS_2.

The structure of $\{[tmdacp]_2Sn\}_2CS_2$---$\{Sn(tmdacp)_2\}$ was solved by single crystal X-ray diffraction and is shown below in Figure 2.4.4.

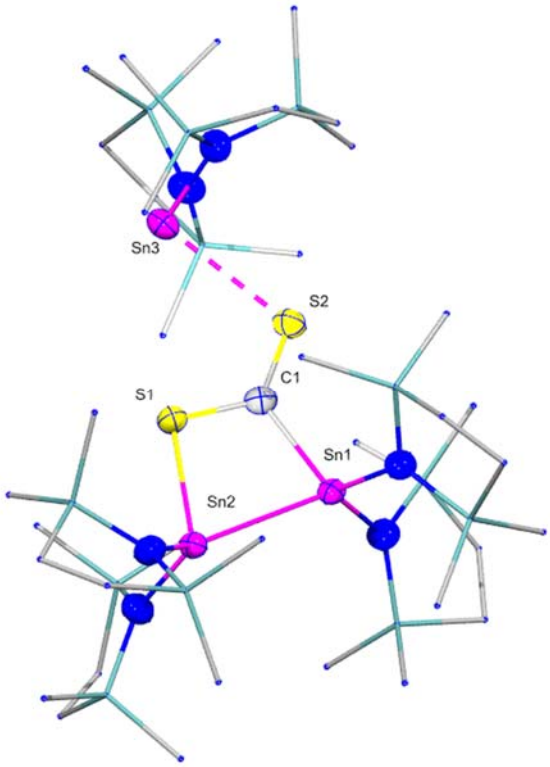

Figure 2.4.4 X-ray structure of {[tmdacp]$_2$Sn}$_2$CS$_2$---{Sn(tmdacp)$_2$}. For clarity, hydrogen atoms are not shown.

This complex can best be described as two molecules of (tmdacp)$_2$Sn bonded to CS_2 through the carbon and one of the sulfur atoms. It is a cluster of three (tmdacp)$_2$Sn molecules coordinated to one CS_2 molecule that has been reduced to $(CS_2)^{2-}$. The S(2)-Sn(3) distance is 3.012 Å and is greater than the sum of covalent radii for Sn and S (1.39 and 1.05 Å respectively). However, this distance is within the van der Waals radii of 3.96 Å and suggests there is some interaction between the sulfur and tin. The interaction can be thought of as a lone pair of electrons from sulfur donating into the empty p-orbital of the stannylene. This extra electron density at Sn(3) can be seen in the upfield shift of ~ 445 ppm in the ^{119}Sn NMR (808 ppm for the free stannylene to 363 for the complex). Aside from the dark green color, which is unusual with main group elements, it is notable that this complex is thermochromic in solution. Upon heating it turns to a dark yellow and then back to dark green at room temperature. This can be repeated many times as long as the solution is kept in a closed system under an inert atmosphere.

In summarizing this work on the reactivity of these two tin(II) silyl amides, [(Me$_3$Si)$_2$N]$_2$Sn and [tmdacp]$_2$Sn, they are essentially electronically identical but their reactivity with the carbon dichalcogenides CO_2, OCS and CS_2 is markedly different, suggesting that sterics play an important role in these reactions. Use of the slightly smaller 2,2,5,5-tetramethyl-2,5-disila-1-aza-cyclopentadienyl ligand provides an overall more reactive tin species, [tmdacp]$_2$Sn. The reaction of [(Me$_3$Si)$_2$N]$_2$Sn with OCS resulted in the cluster Sn$_4$(μ_4-O)(μ_2-OSiMe$_3$)$_5$(η^1-N=C=S).

The reaction of $[tmdacp]_2Sn$ with CO_2 was rapid and yielded a $(\mu_4\text{-}O)Sn_4$ cluster - $Sn_4(\mu_4\text{-}O)(\mu_2\text{-}O_2C[tmdacp]_4)(\mu_2\text{-}N{=}C{=}O)_2$. Two of the tins in the cluster are bound to two N=C=O ligands through the nitrogen atoms, and the complex also contains the first structurally characterized examples of a silyl-substituted carbamate.

The reaction of $[tmdacp]_2Sn$ with OCS was rapid and yielded an intractable solid, while the reaction of $[tmdacp]_2Sn$ with CS_2 yielded $\{[tmdacp]_2Sn\}_2CS_2$--- $Sn[tmdacp]_2$. This is a dark green complex that is thermochromic in solution. It is a cluster of three $(tmdacp)_2Sn$ molecules coordinated to one CS_2 molecule that has been reduced to $(CS_2)^{2-}$. It could loosely be considered a "transition state". The decreased steric congestion around the tin centers has allowed for the complexation of the carbon disulfide moiety to tin atoms but because of the decreased electrophilicity of the carbon in the CS_2 no tin-nitrogen bonds have been broken. In this case there is the beginning of a reaction as opposed to no reaction in the $[(Me_3Si)_2N]_2Sn$ and CS_2 system.

Table 2.4.1 DFT Calculation results (B3LYP/LACVP) for tin silyl amides and comparisons to the solid-state X-ray and gas phase electron diffraction results.**

	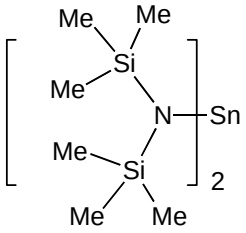 Bis[*N,N'*-bis(trimethylsilyl)amino]tin(II) $[(Me_3Si)_2N]_2Sn$			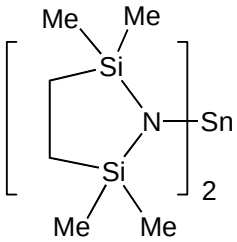 Bis(2,2,5,5-tetramethyl-1-aza-2,5-disilacyclopent-1-yl)tin(II) $(tmdacp)_2Sn$
	DFT	X-ray[27]	Elect. Diff.[28]	DFT
Sn-N bond length	2.09 Å , 2.09 Å	2.096, 2.088 Å	2.09 Å	2.07 Å, 2.07 Å
N-Si bond length	1.77 Å, 1.77 Å, 1.77 Å, 1.77 Å	1.742 Å		1.78 Å, 1.78 Å, 1.78 Å, 1.78 Å
N-Sn-N angle	107.2º	104.7º	96º	107.1º
Si-N-Si angle	120.2º, 120.6º	123 º		109.4º, 109.4º
Si-N-Sn-N dihedral angles	48.2º, 52.4º, 37.3º, 34.6º			43.2º, 44.0º, 22.3º, 21.4º
Ligand cone angle	144.4º, 144.6º			122.8º , 123.1º
Charge on Sn	0.87			0.85
Charge on N	-1.05, -1.05			-1.04, -1.04
Charge on Si	0.89, 0.89, 0.90, 0.90			0.84, 0.84, 0.88, 0.89

Note: For any measurement for which several atoms could be considered, the average measurement given.

2.4.2 Reactivity of Group 2 Silyl Amide Complexes with CO_2

By moving to more electrophilic group 2 metals (Mg, Ca or Ba), we have been able to decrease the reaction time from hours required for the group 14 complexes to minutes.[18] In an attempt to better control the selectivity of the elimination reaction, a series of complexes with the general formula $Mg[NRR']_2(solv)_x$ (solv = ether, THF, pyridine, HMPA or 4-DMAP (Table 2.4.2) were prepared.

Table 2.4.2 Summary of ligands and geometry of magnesium silyl amides.

R	R'	Geometry at Mg	Coordination number at Mg
i-Pr-, $PhCH_2$-, *t*-Bu-, Ph-, $(Me)_3C_6H_2$-, (2,6-(*i*-Pr)$_2$-4-adamantylphenyl)	Me_3Si-	Pseudo-Tetrahedral	4 (two solv)
Adamanyl-, *t*-$BuMe_2Si$-	Me_3Si-	Trigonal	3 (one solv)
c-Hex	Me_3Si-	Trigonal - Dimer	3 (solv free)
c-Hex	*c*-Hex	Trigonal - Dimer	3 (solv free)
t-$BuPh_2Si$-	Me_3Si-	Bent	2 (solv free)

All CO_2 reactions appeared to be complete in 1-3 minutes, and as long as R' = $SiMe_3$, a mixture of both isocyanate R-N=C=O and carbodiimide R-N=C=N-R were obtained. No evidence for the formation of Me_3Si-N=C=O or Me_3Si-N=C=N-$SiMe_3$ was observed. Neither the metal solvation number nor the steric/electronic properties of the alkyl, aryl or silyl substituent had a predictable effect on the product distribution. Only when both R and R' = cyclohexyl was there no elimination. Instead, a carbamate with the formula $[Mg_2(O_2CNCy_2)_4(HMPA)]$ was produced (Figure 2.4.5).[29] This compound exhibited the never-before-seen η^2-chelation mode (Figure 2.4.5) that had been postulated not to exist because of the highly strained four-membered ring.[20]

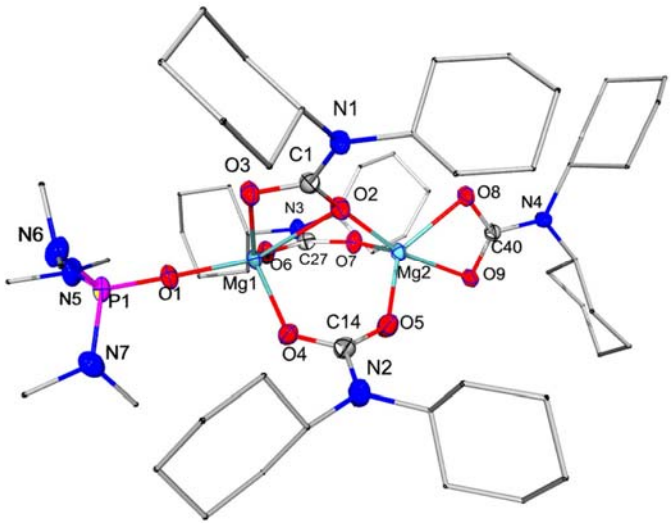

Figure 2.4.5 Structure of $[Mg_2(O_2CNCy_2)_4(HMPA)]$. For clarity, hydrogen atoms and a non-coordinated solvent molecule are not shown.

The four carbamato ligands bind to the two Mg atoms by using three different bonding modes: two of the carbamato groups bind in the μ_2,η^2 fashion, one in the μ_2,η^3 fashion, and one in the previously unknown mode η^2. The Mg(1)-Mg(2) distance of 3.3802 Å is

found to be significantly longer than the Mg-Mg bond distance (3.150 Å) seen in a similar molecule, $[Mg_2(O_2CNPh_2)_4(HMPA)_2]$, but slightly shorter than that seen in the Mg trimers $[Mg_3(O_2C\textit{i}\text{-}Pr)_6(HMPA)_2]$ (3.496 Å) and $[Mg_3(O_2CNMe_2)_6(HMPA)_2]$ (3.459 Å).[20]

The Mg atoms in $Mg_2(O_2CNCy_2)_4(HMPA)$ are found to be dissimilar in the structure, due to the presence of an HMPA solvent molecule coordinated to only one of the Mg atoms. This solvated magnesium atom, Mg(1), is surrounded by two shorter Mg-O bonds (1.951 and 1.96 Å) from the O-donor atoms of the two symmetrical bridging carbamato ligands as well as two longer Mg-O interactions (2.027 and 2.274 Å) from the unsymmetrical chelating carbamato group. The HMPA solvent also coordinates to Mg(1) through the oxygen donor atom O(1). Using the Mg(1)-O(1) bond as the point of the pyramid, it can be seen that the Mg-(1) atom adopts a very distorted square pyramidal structure using the four oxygen atoms of the carbamato groups, with the one longer Mg(1)-O(2) bond from the unsymmetrical binding mode adding further to the distortion around Mg. The other Mg atom, Mg(2), is surrounded by five O-donor atoms of the various carbamato ligands.

It is important to note that in the geometry around Mg(2) is seen the first example of a terminal bidentate carbamato ligand bound to a Mg atom in an η^2 mode. The two symmetrically bridging carbamato linkages bind to Mg(2) exactly as is seen with Mg(1), with identical bond Mg-O lengths resulting in both cases. The unsymmetrically bridging carbamato group is bound to Mg(2) via O(2), and, as was seen with Mg-(1), the Mg(2)-O(2) bond length from this unsymmetrically bound ligand is lengthened relative to the Mg-O bonds of the symmetrically bound carbamato ligands (2.013 versus 1.959 and 1.944 Å). As we noted, Mg(2) has additionally a terminal bidentate (η^2) carbamato ligand bound through O(8) and O(9). In this complex, the Mg(2)-O(8) and Mg(2)-O(9) bond lengths of 2.041 and 2.108 Å, respectively, are longer than the Mg-O bonds seen in the μ_2,η^2 bonding mode for Mg(1)-O(5) and Mg(1)-O(7) (1.959 and 1.944 Å). The O(8)-Mg(2)-O(9) bond angle of 64.18° is quite similar to the N-Mg-N bond angles of 62.3-65.6° seen in related terminal bidentate Mg carbodiimides.

In addition to the magnesium complexes described in Table 2.4.2, the compound $Mg(tmdacp)_2(Et_2O)_2$ was prepared, in order to compare its reactivity with $Mg[N(SiMe_3)_2]_2$, as was done with the corresponding tin complexes in the previous section. Crystalline $Mg(tmdacp)_2(Et_2O)_2$ was placed in an NMR tube inside a stainless steel high pressure reactor. The reactor was then pressurized with CO_2 to 700 psig. After five hours, the system was depressurized and a solid product was isolated (Scheme 2.4.5). IR spectroscopic studies of the solid clearly indicated that a reaction had occurred. The IR spectrum exhibited ν(C-O) stretching vibrations at 1614 and 1529 cm^{-1} that are assigned to the asymmetric ν_{as}(C-O) and symmetric ν_s(C-O) stretching modes. The stretches clearly suggest that the insertion product is formed.

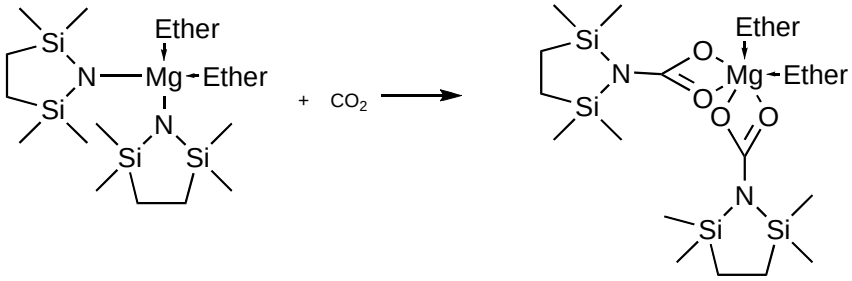

Scheme 2.4.5 Solid-gas reaction of $Mg(tmdacp)_2(Et_2O)_2$ with CO_2.

In order to more completely characterize the reaction product, it was dissolved in pyridine and allowed to sit overnight. The resulting crystals were analyzed by X-ray diffraction and found to be $Mg(NCO)_2(py)_5$. The IR spectrum of the crystalline product showed asymmetric stretching N=C=O stretching vibrations at 2227 and 2199 cm^{-1}. The supernatant pyridine solution was analyzed by GC-MS. The GC-MS indicates the production of the corresponding siloxane with no evidence of isocyanate or carbodiimide formation. A proposed reaction mechanism is seen in Scheme 2.4.6 below. It is dependent on the inherent proximity of the isocyanate produced from the initial elimination after CO_2 insertion and the newly formed metal-oxygen bond.

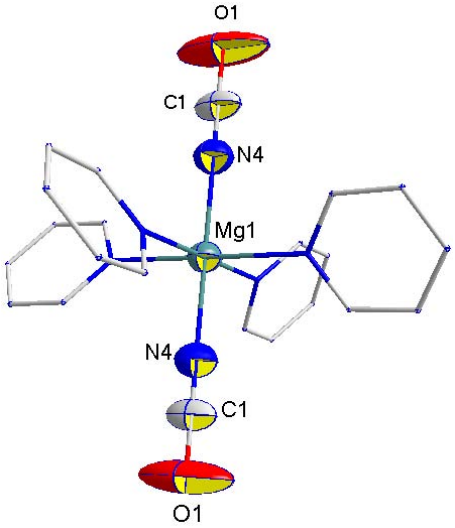

Figure 2.4.6 X-ray structure of $Mg(NCO)_2(py)_5$. For clarity, hydrogen atoms and one molecule of non-coordinating pyridine are not shown.

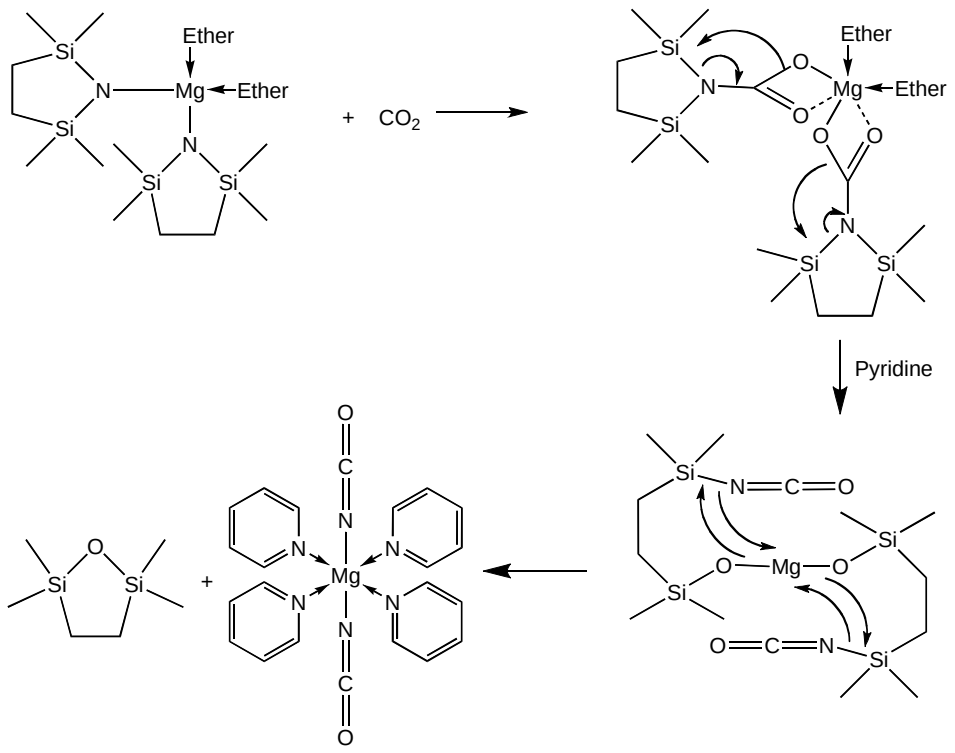

Scheme 2.4.6. Proposed mechanism for the formation of $Mg(NCO)_2(py)_5$.

2.4.3 Reactivity of Group 2 and 12 Phosphino Amide Complexes with CO_2

Because the driving force behind the isocyanate/carbodiimide elimination reaction is the formation of a strong Si-O bond in the metal-containing product, we became curious about whether the P-O bond, which is also very strong, would provide a similar driving force. Therefore, we began to explore the reactivity of phosphino-substituted amides. The series of group 2 compounds $M[N(i\text{-}Pr_2P)(SiMe_3)]_2(THF)_x$ (M = Mg, Ca, Sr) was prepared according Scheme 2.4.7 and characterized by X-ray crystallography (Figure 2.4.7). As expected, the primary coordination was through nitrogen, with a weak metal-phosphorus interaction present in the solid state. The metal coordination sphere was completed by one (Mg) or two (Ca, Sr) molecules of THF solvent.

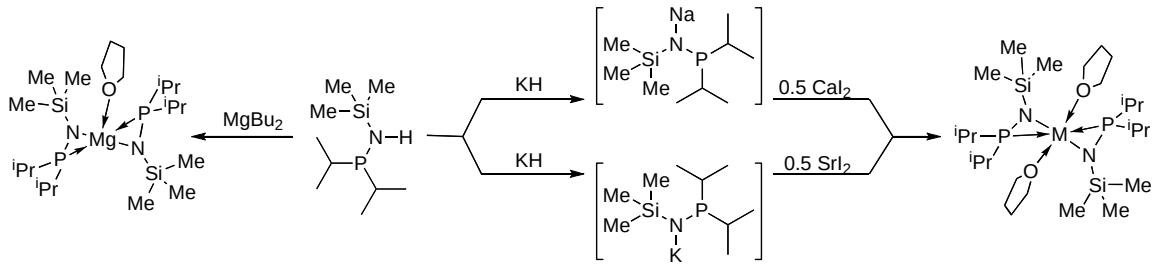

Scheme 2.4.7 Synthesis of $M[N(i\text{-}Pr_2P)(SiMe_3)]_2(THF)_x$ (M = Mg, Ca, Sr).

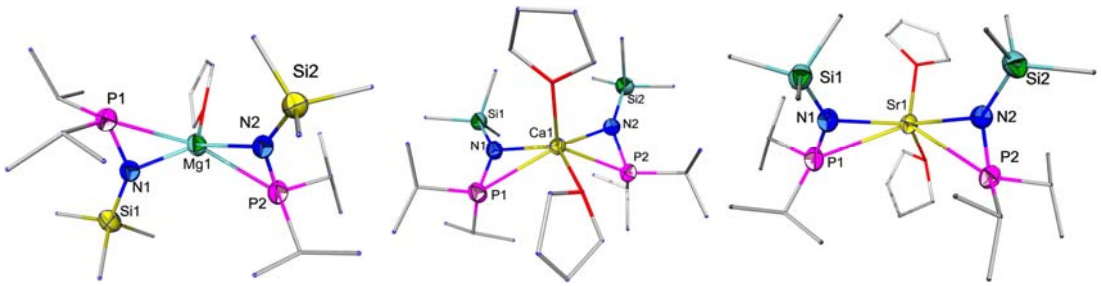

Figure 2.4.7 X-ray structures of M[N(*i*-Pr$_2$P)(SiMe$_3$)]$_2$(THF)$_x$ (M = Mg, Ca, Sr). For clarity, hydrogen atoms are not shown.

These complexes were dissolved in hexanes and exposed to one atmosphere of carbon dioxide for 15 minutes at room temperature (Scheme 2.4.8). Subsequent analysis by GC-MS, IR and ^{31}P NMR spectroscopy showed complete, exclusive conversion to the phosphino-substituted isocyanate *i*-Pr$_2$P-N=C=O. This was somewhat surprising given the mixture of products obtained when alkyl, aryl or other silyl groups were used instead of the phosphino substituent.

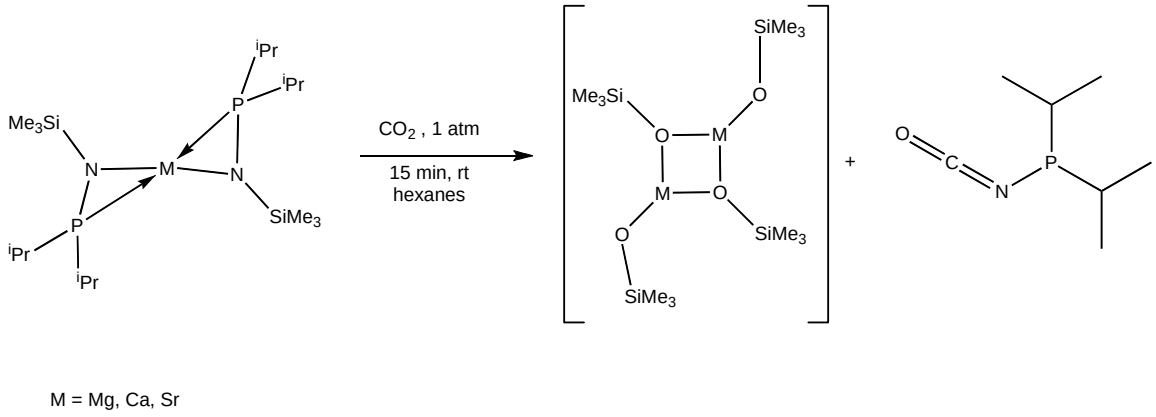

M = Mg, Ca, Sr

Scheme 2.4.8 Reaction of M[N(*i*-Pr$_2$P)(SiMe$_3$)]$_2$(THF)$_x$ (M = Mg, Ca, Sr) with CO$_2$.

Attempts to synthesize an analogous group 12 complex resulted instead in the formation of the monosubstituted alkylzinc amide shown below (Scheme 2.4.9). X-ray crystallographic studies show that in the solid state this molecule forms a dimer via a Zn---P dative bond (Figure 2.4.8), but it is likely monomeric in solution. Because this molecule contains only a single metal-amide bond, carbodiimide formation would not be possible, and exclusive formation of R$_2$P-N=C=O was anticipated upon reaction with carbon dioxide.

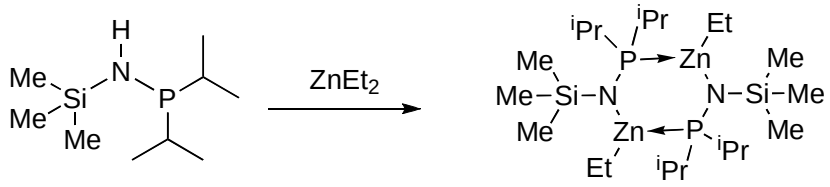

Scheme 2.4.9 Synthesis of {EtZn[N(*i*-Pr$_2$P)(SiMe$_3$)]}$_2$.

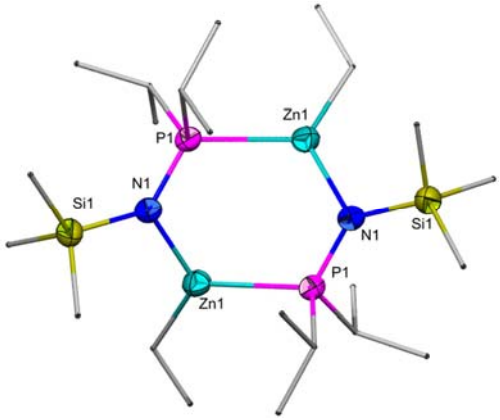

Figure 2.4.8 X-ray structure of {EtZn[N(*i*-Pr$_2$P)(SiMe$_3$)]}$_2$. For clarity, hydrogen atoms are not shown.

Carbon dioxide was bubble through a hexanes solution of EtZn[N(*i*-Pr$_2$P)(SiMe$_3$)]}$_2$ for 15 minutes at room temperature (Scheme 2.4.10). Surprisingly, isocyanate was not observed by GC-MS analysis of the resultant solution, and the reason for this was revealed by X-ray crystallographic analysis of the solid products. Two different products, whose ratio varies with reaction time and concentration, were isolated. The colorless, block-shaped crystals **A** (Figure 2.4.9) were found to have CO_2 coordinated in a zwitterionic fashion to the phosphorus atom of the ligand. The reasons for this type of interaction instead of the typical insertion into the metal-amide bond are not immediately clear, but similar coordination was subsequently observed in model studies with the heavier CO_2 analog CS_2 (vide infra) and in a recent paper by Stephan *et al.* on CO_2 coordination by frustrated Lewis pairs.[30]

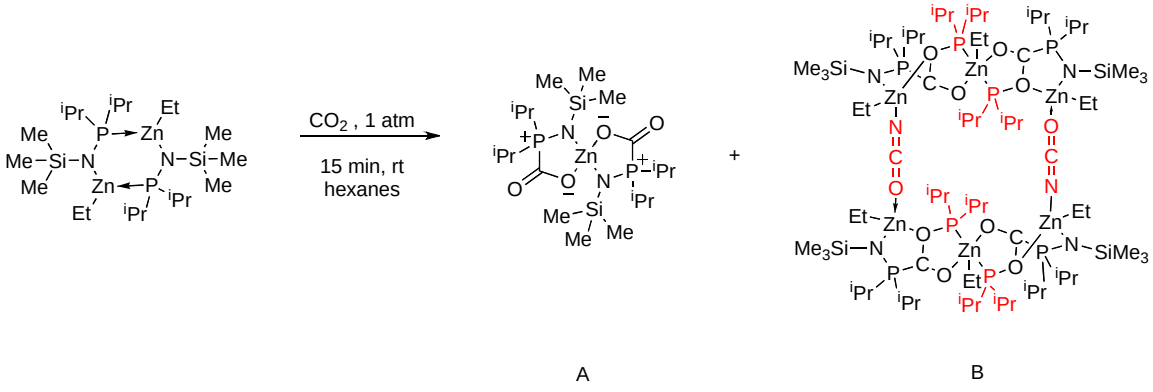

Scheme 2.4.10 Reaction of {EtZn[N(*i*-Pr$_2$P)(SiMe$_3$)]}$_2$ with CO_2.

The rod-shaped, colorless crystals **B** (Figure 2.4.10) also isolated from this reaction showed the same coordination motif as **A** in the corners of the hexanuclear complex. The complex also contained what appear to be fragments of the expected isocyanate, highlighted in red in Scheme 2.4.10. Cleavage of the isocyanate P-N bond gives the R$_2$P- and –N=C=O moieties that are coordinated to the central and corner Zn atoms, respectively. The lack of an ethyl group on the Zn atoms in **A** and the [Zn(OSiMe$_3$)] fragment that must be formed in order to produce the isocyanate cleaved in **B** indicate

that more products must be present in this reaction than have so far been identified. The reaction pathway leading to these two complexes is still under investigation.

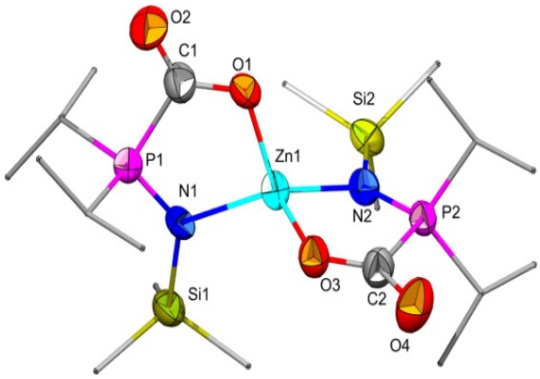

Figure 2.4.9 X-ray structure of the block-shaped crystals A from the reaction of $\{EtZn[N(i\text{-}Pr_2P)(SiMe_3)]\}_2$ with CO_2. For clarity, hydrogen atoms are not shown.

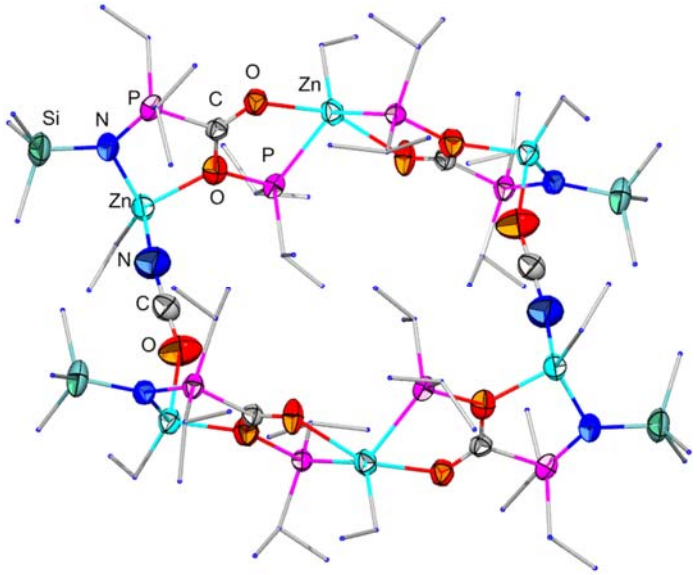

Figure 2.4.10 X-ray structure of the rod-shaped crystals B from the reaction of $\{EtZn[N(i\text{-}Pr_2P)(SiMe_3)]\}_2$ with CO_2. For clarity, hydrogen atoms are not shown.

As noted above, we expanded our studies of divalent metal complexes of silyl-substituted amides to also include phosphino-substituted amides with the belief that the P-O bond would provide enough of a driving force for the elimination of isocyanates and/or carbodiimides. Thus, we prepared the known complexes $M[N(PPh_2)_2]_2(THF)_3$ (M = Ca, Sr),[31,32] which contain no silyl groups. Bubbling an excess of dry CO_2 at room temperature through a solution of $M[N(PPh_2)_2]_2(THF)_3$ in THF led to a rapid reaction, as evidenced by the complete disappearance of the ^{31}P NMR signal of the starting material in less than 15 minutes (Scheme 2.4.11).[33] ^{31}P NMR analysis of the product solution indicated a mixture of P-containing compounds. Easily identifiable by their ^{31}P NMR chemical shifts were $Ph_2P\text{-}Ph_2P{=}N\text{-}PPh_2$, a compound prepared previously by Nöth[34]

using a direct synthesis, and trace amounts of $N(PPh_2)_3$.[35] It was thus obvious to us that the expected reaction to form isocyanate or carbodiimide had not occurred, or at least not cleanly.

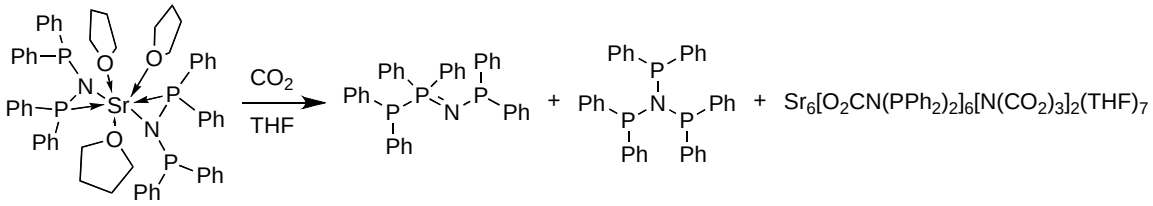

Scheme 2.4.11 Reaction of $Sr[N(PPh_2)_2]_2(THF)_3$ with CO_2.

Upon prolonged standing, the reaction mixture deposited colorless, single crystals. X-ray diffraction studies revealed the formation of $Sr_6[O_2CN(PPh_2)_2]_6[N(CO_2)_3]_2(THF)_7$ (Figure 2.4.11). Immediately apparent are several interesting structural features. The molecule consists of a hexanuclear strontium backbone held together by six novel bridging phosphino-modified carbamate ligands, $-O_2CN(PPh_2)_2$ formed by CO_2 insertion into the Sr-N bond of a $-N(PPh_2)_2$ ligand. While the primary bonding mode of the new ligand is η^2-chelating to Sr via the O-C-O linkage of the carbamate, one of the O atoms also acts as a bridge to an adjacent Sr atom. Similarly, one of the P atoms of the ligand provides an additional chelating arm to the same adjacent Sr atom in the Sr_6 backbone. This connectivity is repeated around the ring. The Sr_6 backbone itself can be visualized as the chair form of cyclohexane. As well, one molecule of THF is also coordinated to each Sr atom, and one additional THF molecule is present but disordered within the crystal lattice.

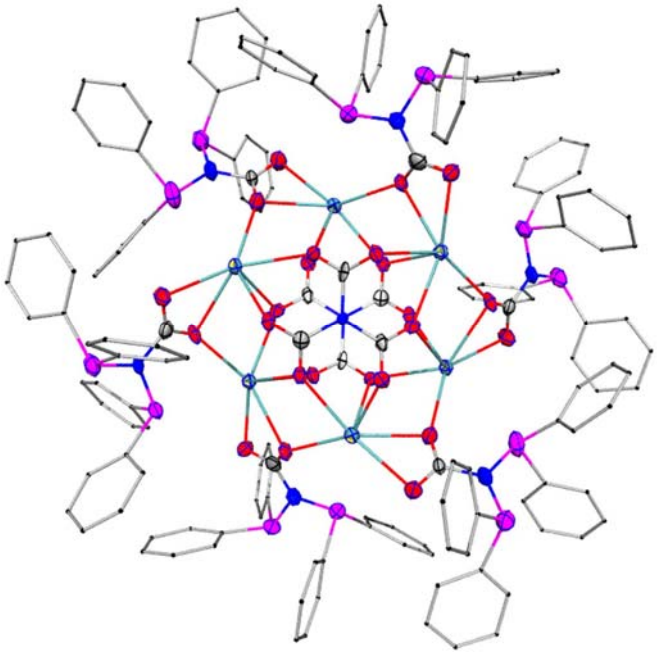

Figure 2.4.11 X-ray structure of $Sr_6[O_2CN(PPh_2)_2]_6[N(CO_2)_3]_2(THF)_7$. For clarity, hydrogen atoms and THF solvent are not shown. Sr = green, P = purple, N = blue, O = red, C = grey.

The atomic structure of the core is shown in more detail in Figure 2.4.12. Remarkably, two -$N(PPh_2)_2$ ligands have reacted with CO_2 to cleave the -PPh_2 groups from nitrogen and formally insert three molecules of CO_2, resulting in the formation of two unprecedented, symmetry-related $[N(CO_2)_3]^{3-}$ ligands linked to the Sr_6 backbone. A thorough literature search turned up no other molecules containing the $[N(CO_2)_3]^{3-}$ fragment.

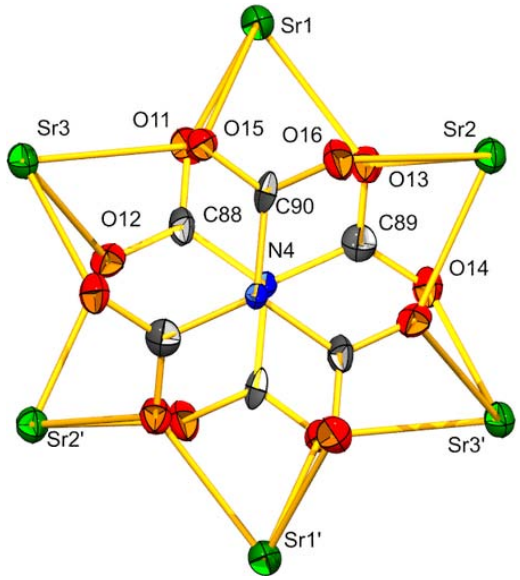

Figure 2.4.12 Central core of $Sr_6[O_2CN(PPh_2)_2]_6[N(CO_2)_3]_2(THF)_7$, showing the $[N(CO_2)_3]^{3-}$ anions.

The extraordinary reactivity of $Sr_6[O_2CN(PPh_2)_2]_6[N(CO_2)_3]_2(THF)_7$ towards CO_2, resulting in facile CO_2-induced cleavage of the -$N(PPh_2)_2$ ligand at ambient temperature and pressure within a matter of minutes, is highly unexpected and unusual. $[N(CO_2)_3]^{3-}$ can be viewed as the trianion derived from deprotonation of the hypothetical $N(CO_2H)_3$ molecule. While the parent triprotic acid complex is unknown, organic esters of the formula $N(CO_2R)_3$, where R = Et, *t*-Bu, or substituted cyclohexyl derivatives, have been prepared by traditional synthetic routes that do not involve direct insertions of CO_2.[36-38]

The parent $Sr[N(PPh_2)_2]_2(THF)_3$ "fixes" 12 molecules of CO_2 into two new ligands – a phosphino-substituted carbamate as well as the completely unknown $[N(CO_2)_3]^{3-}$ ligand under extremely mild conditions – room temperature, atmospheric pressure, and in a matter of a few minutes! This ligand has "glued" together three molecules of CO_2 with one N atom! While Sr is not the metal we would choose due to expense, we have demonstrated *the same chemistry with Ca*, which is much cheaper. This result is exceedingly important as it demonstrates our original concept of using metal ions for complexation of CO_2 is feasible.

2.4.4 Reactivity of Group 2 and 12 Phosphino Amide Complexes with CS_2

In order to gain additional insight into the diverse reaction pathways of the heavier CO_2 analog CS_2 with divalent metal amides, we carried out studies of several of the group 2 and 12 complexes described in the preceding section. Reaction of the group 2 complexes $M[N(PPh_2)_2]_2(THF)_3$ (M = Ca, Sr)[31,32] with excess CS_2 (Scheme 2.4.12) gave very different results from the related reactions with CO_2, which were described above. Instead of insertion into the M-N bond or fixation multiple equivalents of CE_2 around a nitrogen atom, the isolated product instead showed cleavage of the CS_2 to form a P=S double bond in the ligand with formal loss of "CS". Unlike CO, CS is not stable as a free molecule, and its fate has not yet been determined. This splitting induced a change in coordination to chelation through sulfur instead of monodentate N-coordination. Transition metals have long been known to split CS_2 in this manner, but this reactivity *has never before been seen in main group elements.*

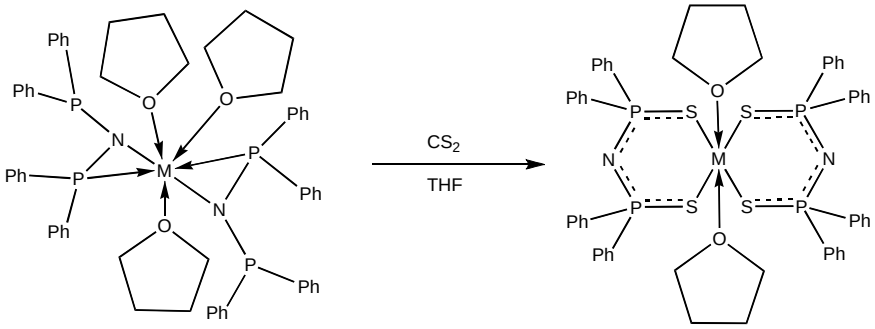

Scheme 2.4.12 Reaction of $M[N(PPh_2)_2]_2(THF)_3$ (M = Ca or Sr) with CS_2.

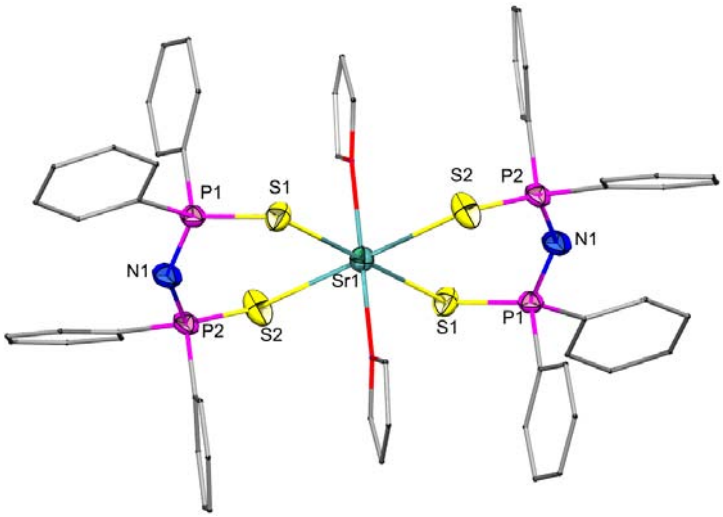

Figure 2.4.13 X-ray structure of $Sr\{N[P(=S)Ph_2]_2\}_2(THF)_2$. For clarity, hydrogen atoms are not shown.

The group 12 complex $\{EtZn[N(PPh_2)_2]\}_2$ was reacted with CS_2 under similar conditions. X-ray crystallographic analysis of the product revealed similar reactivity as in the group 2 $M[N(PPh_2)_2]_2$ complexes. Carbon disulfide was again split to form a P=S double bond, with change of ligand coordination to S,S-chelation. As with the group 2 metal complexes, the fate of the "CS" has not yet been determined. Understanding the discrepancy in metal-to-ligand stoichiometry between the starting material and product is also still underway.

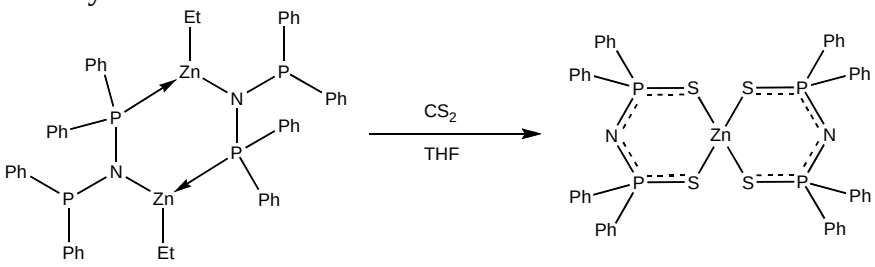

Scheme 2.4.13 Reaction of $\{EtZn[N(PPh_2)_2]\}_2$ with CS_2.

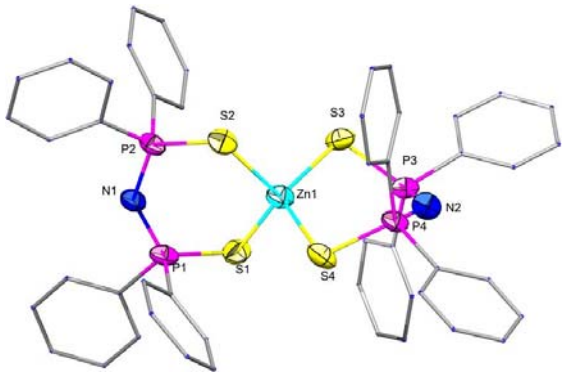

Figure 2.4.14 X-ray structure of $Zn\{N[P(=S)Ph_2]_2\}_2$. For clarity, hydrogen atoms are not shown.

The compounds $M[N(i\text{-}Pr_2P)(SiMe_3)]_2(THF)_x$ (M = Mg, x = 1; M = Ca, x = 2) also split CS_2 (Scheme 2.4.14). The presence of only one phosphorus atom in the –N(*i*-Pr_2P)($SiMe_3$) ligand made S,S-chelation impossible, and X-ray crystallographic studies showed that the M-N bond remained intact (Figure 2.4.15). In all the group 2 and 12 complexes, the reactions were extremely fast. The solutions showed dramatic color changes (usually bright red) within seconds of the CS_2 addition. This suggests that despite the lack of literature precedent, this splitting reaction is not limited to specialized systems.

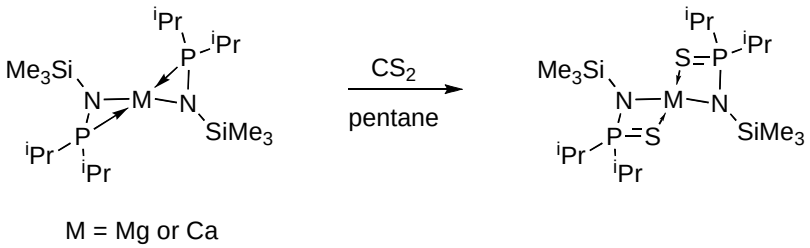

M = Mg or Ca

Scheme 2.4.14 Reaction of $M[N(i\text{-}Pr_2P)(SiMe_3)]_2(THF)_x$ with CS_2.

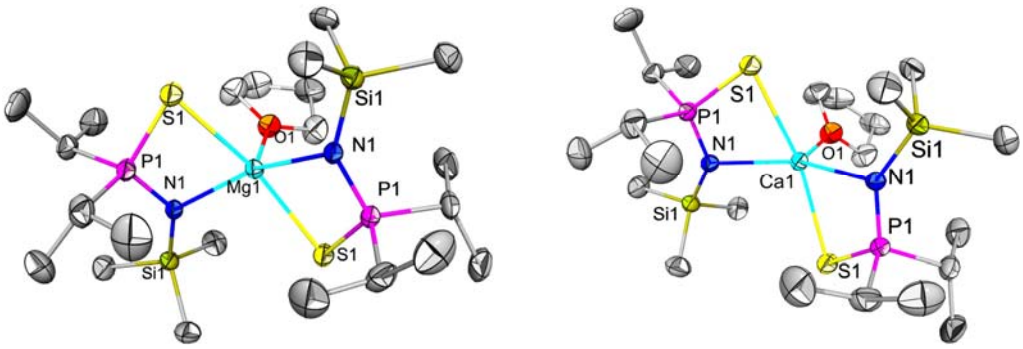

Figure 2.4.15 Structures of M{N[*i*-Pr$_2$P(=S)](SiMe$_3$)}$_2$(THF) (M = Mg or Ca). For clarity, hydrogen atoms are not shown.

2.4.5 Reactions of Phosphino Amine Ligands with CS_2

The observation that in some cases the metal-amide bond remained intact despite the splitting of CS_2 prompted us to question whether the metal was necessary for the activation. Reaction of a THF solution of $HN(PPh_2)_2$[34] with CS_2 at room temperature immediately produced a deep red solution (Scheme 2.4.15). Analysis by ^{31}P NMR showed a complex mixture of products, the most abundant of which was isolated and characterized by single crystal X-ray diffraction. As Figure 2.4.16 shows, the product can be considered a dimer of the ligand formed in the reaction of the related group 2 complexes. One P=S double bond remained intact while the other formed a disulfide bond with a second identical molecule. As in the metal complexes, a formal equivalent of "CS" is lost for each phosphorus atom.

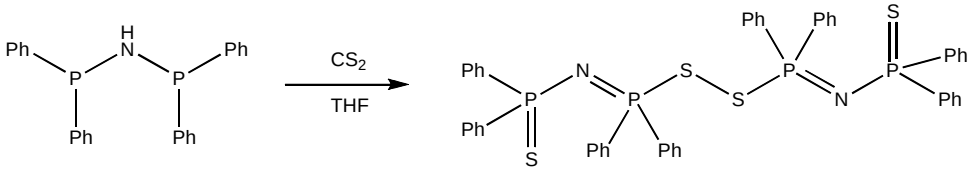

Scheme 2.4.15 Reaction of HN(PPh$_2$)$_2$ with CS$_2$.

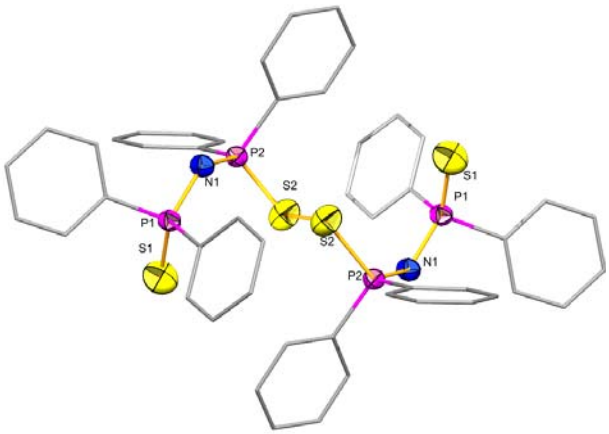

Figure 2.4.16 X-ray structure of [Ph$_2$P(=S)N=P(Ph)$_2$S]$_2$. For clarity, hydrogen atoms are not shown.

Surprisingly, this type of reactivity was not continued in the reaction of HN(*i*-$Pr_2P)_2$ with CS_2 (Scheme 2.4.16). Instead, a crystalline red CS_2 adduct was isolated as the only product. Close examination of the ^1H and ^{31}P NMR spectra revealed that only one of the two phosphorus atoms had reacted, producing a molecule with the formula (*i*-Pr_2PH)N=[P(*i*-$Pr)_2(CS_2)$]. The structure was confirmed crystallographically (Figure 2.4.17).

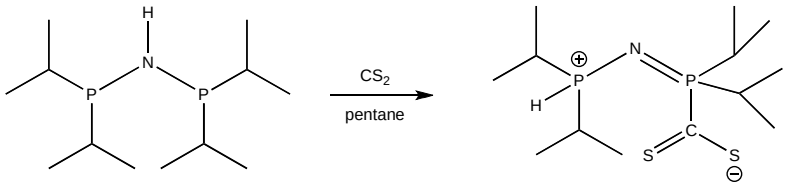

Scheme 2.4.16 Reaction of HN(*i*-$Pr_2P)_2$ with CS_2.

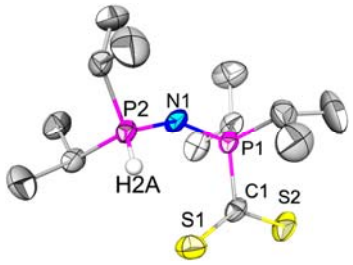

Figure 2.4.17 X-ray structure of *i*-$Pr_2PH)N=[P(i\text{-}Pr)_2(CS_2)]$. For clarity, hydrogen atoms, except for the P-H, are not shown.

The reaction of HN(*i*-Pr_2P)($SiMe_3$) with CS_2 behaved similarly to that of HN(*i*-$Pr_2P)_2$, although without the tautomerization. Instead, a simple P-C zwitterionic adduct reminiscent of the CO_2 product of this ligand's Zn complex (Figure 2.4.9) was the only product observed. This compound was isolated as dark red crystals and characterized by ^{31}P NMR spectroscopy and X-ray crystallography.

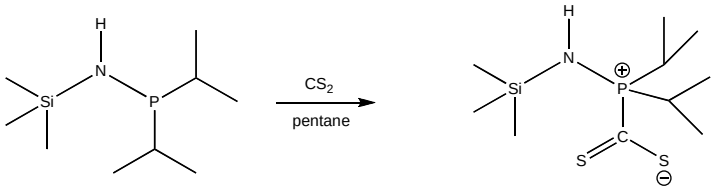

Scheme 2.4.17 Reaction of HN(*i*-Pr_2P)($SiMe_3$) with CS_2.

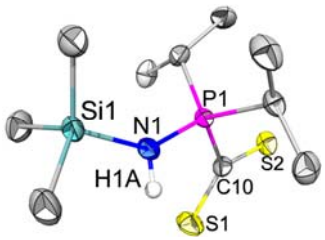

Figure 2.4.18 X-ray structure of HN[*i*-$Pr_2P(CS_2)$]($SiMe_3$). For clarity, hydrogen atoms are not shown.

3 EXPERIMENTAL

3.1 General experimental

All manipulations were carried out in an argon-filled glove box or by using standard Schlenk techniques for air sensitive compounds. Anhydrous solvents were purchased from Aldrich or the Fischer Scientific Company, after which they were stored in the glove box if the synthesis required dry, oxygen free solvents. ^{1}H, and $^{13}C\{^{1}H\}$, $^{31}P\{^{1}H\}$ and $^{119}Sn\{^{1}H\}$ NMR spectra were obtained on a Bruker AMX 250 spectrometer and were referenced to residual solvent downfield of $SiMe_4$ (^{1}H and $^{13}C\{^{1}H\}$), external H_3PO_4 ($^{31}P\{^{1}H\}$) or $SnMe_4$ ($^{119}Sn\{^{1}H\}$). X-ray data were collected on a Bruker X8 Apex2 CCD-based X-ray diffractometer equipped with an Oxford Cryostream 700 low temperature device and normal focus Mo-target X-ray tube (λ = 0.71073 A) operated at 1500 W power (50 kV, 30 mA). Structures were solved using the SHELX software suite (version 6.1). All non-hydrogen atoms were refined anisotropically and hydrogen atoms were included as riding on their respective heavy atoms. Figures were prepared using Diamond 3.1f. GC-MS data were obtained on a Hewlett-Packard Model 5890/5972A Series. IR spectra were recorded on a Bruker Vector 22 MIR spectrometer. Elemental analyses were performed at Columbia Analytical Services, Inc., 3860 S. Palo Verde Road, Tucson, Arizona 85714.

3.2 Synthesis and Characterization

3.2.1 Dialkyl Dimethoxy Tin Complexes

Synthesis of di-octyl dimethoxy tin: To di-octyl tin dichloride (20.44 g; 0.049 mol) in ether (~250 mL) was added MeONa (2.27 g of Na; 0.049 mol in methanol 10 g) drop wise. The reaction was allowed to stir for several hours and the NaCl filtered off. The solvents were removed under vacuum to give 20 g of crude product ($octyl_2Sn(OMe)_2$). The crude product was distilled on a short path column under vacuum (~25 μHg) and pure $octyl_2Sn(OMe)_2$ was collected between 148 – 155 ºC (12.7 g; 64% yield). ^{1}H NMR (C_6D_6); δ 3.69 (OCH_3, 6H), 1.81 (mult., 3H), 1.30 (mult. 25 H), 0.91 (mult. 6 H). $^{13}C\{^{1}H\}$(C_6D_6); δ 52.41 (OCH_3), 34.53, 32.39, 29.80, 29.77, 25.80, 23.14, 19.89 (CH_3), 14.38 (CH_2Sn). ^{119}Sn (C_6D_6); δ -163 compared to -160 for $Bu_2Sn(OMe)_2$.

Reaction of CO_2 and methanol in the presence of di-octyl dimethoxy tin: Di-octyl dimethoxy tin (1.6 g; 4 mmol) was mixed with methanol (24 g; 30.3 mL) to give a 0.13 M solution of Sn in methanol. This solution was transferred to a 100 cc Parr reactor under an inert atmosphere of argon. The reactor was connected to a source of CO_2 it was slowly heated to a temperature of 155 °C. The CO_2 was compressed using a Whitey compressor into the reactor to give a pressure of ~2100 psig. The reaction was stirred for 18 hrs at 155 °C. The reactor was carefully vented and the contents transferred to a vial. Aliquots were removed and analyzed by GC-MS. It was found that ~0.13% of dimethyl carbonate was contained in the reaction mixture along with a white precipitate (oligomers of di-octyl tin oxide).

3.2.2 Cyclams and Metal Cyclam Complexes

Synthesis of zinc(II)-1,4,8,11-tetraazacyclotetradecane bis(perchlorate) – cyclam Zn^{2+}[14]-aneN$_4$ [ClO_4^-]$_2$: For a typical preparation of Zn^{2+}[14]-aneN$_4$ [ClO_4^-]$_2$ the method of Kato and Ito is followed. The cyclam $^{+}$[14]-aneN$_4$ (0.50 g; 2.5 mmol) was dissolved in methanol (~.25 mL). In a separate vial zinc(II) bis(perchlorate) hexahydrate (0.931 g; 2.5 mmol) was dissolved in methanol (7.5 mL). The zinc solution was added slowly to the cyclam solution. During the addition of the zinc perchlorate solution the reaction will turn cloudy. The Zn^{2+}[14]-aneN$_4$ [ClO_4^-]$_2$ solution was usually not isolated but used as is.

Synthesis of zinc(II)-1-(pyridin-2-ylmethyl)-1,4,8,11-tetraazacyclotetradecane bis(perchlorate) – Zn^{2+} 2-methylpyridine-cyclam [ClO_4^-]$_2$: The 1-(pyridin-2-ylmethyl)-1,4,8,11-tetraazacyclotetradecane cyclam (0.175 g; 0.600 mmol) was dissolved in methanol (5.5 g). To this pale yellow solution was added a solution of Zn[ClO_4]$_2$•6H$_2$O (0.224 g; 0.600 mmol) in methanol (4.2 g). The zinc perchlorate/methanol solution was added drop-wise to the 2-methyl-pyridine cyclam solution. After approximately 2/3^{rds} of the way through the addition the reaction mixture turned cloudy. Isolated 0.142 g (43%) for the metal complex as a pale tan solid. The complex can be recrystallized from hot methanol and allowed to slowly cool to room temperature over several hours. Elemental analysis for $C_{16}H_{29}N_5ZnO_8Cl_2$ (Mw = 555.80): C, 34.57; H, 5.27; N, 12.60. Found: C, 34.54; H, 5.06; N, 12.39.

Synthesis of zinc(II)-1-(pyridin-3-ylmethyl)-1,4,8,11-tetraazacyclotetradecane bis(perchlorate) – Zn^{2+} 3-methylpyridine-cyclam [ClO_4^-]$_2$: The 1-(pyridin-3-ylmethyl)-1,4,8,11-tetraazacyclotetradecane cyclam (0.251 g; 0.861 mmol) was dissolved in methanol (2.4 g). To this pale yellow solution was added a solution of Zn[ClO_4]$_2$•6H$_2$O (0.326 g; 0.875 mmol) in methanol (~3 g). The zinc perchlorate/methanol solution was added drop-wise to the 3-methyl-pyridine solution. Similar to the previous preparation using the 2-methyl-pyridine cyclam after approximately 2/3^{rds} of the way through the addition the reaction mixture turned cloudy with microfine crystals. The solution was centrifuged and the clear yellow supernatant with some suspended microfine crystals were removed to another vial. The clear yellow solution with the microfine crystals was heated on a hot water bath to dissolve the fine crystals and allowed to slowly cool to room temperature. After numerous attempts crystals were finally isolated. Due to various attempts at obtaining crystals no yields can be reported. An attempt to obtain a melting point of the pale yellow crystals was above the upper heating point of the oil bath melting point unit (~270 °C). The crystals turned dark yellow amber at 270 °C. Once the product crystallized out of solution it was almost impossible to get it back in again. This precluded obtaining ^{1}H and ^{13}C{^{1}H} spectra due to insolubility. The product behaved very much like a polymeric material.

Synthesis of cadmium(II)-1-(pyridin-2-ylmethyl)-1,4,8,11-tetraazacyclotetradecane bis(perchlorate) – Cd^{2+} 2-methylpyridine-cyclam [ClO_4^-]$_2$: The 1-(pyridin-2-ylmethyl)-1,4,8,11-tetraazacyclotetradecane cyclam (0.111 g; 0.381 mmol) was dissolved

in methanol (3.6 g). To this pale yellow solution was added a solution of $Cd[ClO_4]_2 \cdot 6H_2O$ (0.160 g; 0.381 mmol) in methanol (3 g). The cadmium perchlorate/methanol solution was added drop-wise to the 2-methyl-pyridine cyclam solution. The reaction mixture eventually turned cloudy. X-ray quality crystals were isolated from methanol at -22 °C.

Synthesis of 1,4,8,11-(tetrakis-trimethylsilyl)-1,4,8,11-tetraazacyclotetradecane: The parent cyclam (0.196 g; 0.983 mmol) was slurried in THF (35 g), then cooled to -78 °C. To this solution was added *n*-BuLi (2.5 mL; 1.6 M; 3.9 mmol) drop-wise. The reaction was allowed to stir for 20 mins then warmed to 0 °C 1 hr. The creamy off-white solution was cooled to -78 °C and to this was added Me_3SiCl (0.5 mL; 3.93 mmol) drop-wise. The reaction was allowed to stir while warming to room temperature overnight. The THF was removed under vacuum to give a semi-solid crude product, which was taken up in hexanes and filtered to remove the LiCl. The hexanes were slowly removed during which time the product crystallized as a pale yellow slightly waxy solid. The product was recrystallized from toluene to give a higher purity material.

Synthesis of cadmium(II)-1-(pyridin-3-ylmethyl)-1,4,8,11-tetraazacyclotetradecane bis(perchlorate) – Cd^{2+} 3-methylpyridine-cyclam $[ClO_4^-]_2$: The 1-(pyridin-3-ylmethyl)-1,4,8,11-tetraazacyclotetradecane cyclam (0.132 g; 0.453 mmol) was dissolved in methanol (2.5 g). To this pale yellow solution was added a solution of $Cd[ClO_4]_2 \cdot 6H_2O$ (0.190 g; 0.453 mmol) in methanol (~5 g). The cadmium perchlorate/methanol solution was added drop-wise to the 3-methyl-pyridine cyclam solution. At about half way through the addition the reaction mixture turned cloudy. The solution was centrifuged and the clear yellow supernatant was decanted off. Several methods to isolate a product from the clear yellow solution failed.

Synthesis of mercury(II)-1-(pyridin-2-ylmethyl)-1,4,8,11-tetraazacyclotetradecane bis(perchlorate) – Hg^{2+} 2-methylpyridine-cyclam $[ClO_4^-]_2$: The 1-(pyridin-3-ylmethyl)-1,4,8,11-tetraazacyclotetradecane cyclam (0.104 g; 0.036 mmol) was dissolved in methanol (2.5 g). To this pale yellow solution was added a solution of $Hg[ClO_4]_2 \cdot 3H_2O$ (0.162 g; 0.036 mmol) in methanol (~5 g). The mercury perchlorate/methanol solution was added drop-wise to the 2-methyl-pyridine cyclam solution. At about half way through the addition the reaction mixture turned cloudy. The solution was centrifuged and the clear colorless supernatant was transferred into a separate vial. Low quality crystals were grown over a long period at -22 °C. The ^1H NMR was consistent with the zinc and cadmium complexes.

Synthesis of 1-propionitrile-1,4,8,11-tetraazacyclotetradecane (cyclam-1PN): The 1,4,8,11-tetraazacyclotetradecane cyclam (1.00 g; 5.0 mmol) was dissolved in $CHCl_3$ (~30 mL). To this solution was added acrylonitrile (0.21 g; 4.0 mmol). The reaction was stirred ~86 hrs. The volatiles were removed on a rotovap and dried further at 20 μHg for 45 mins. Collected 1.04 g of an off white solid (mp = 146 – 160 °C). A silica gel column (1 cm x 42 cm) was prepared (Acros, silica gel ultra pure, 60 – 200 μm, 60Å). A mixture of $CHCl_3$:MeOH:i-prNH_2 10:1:1 by volume was prepared and about 30 g of silica gel was slurried in ~90 mL of the solvents. The crude cyclam-1PN was dissolved

in a minimum amount of the solvents and placed on the column. The product was eluted as a yellow oil. Upon standing the yellow oil crystallizes to form clear colorless needles. The structure of this cyclam-1PN was determined by X-ray diffraction.

3.2.3 Heterogeneous catalysts

Preparation of nano(Cu-Ni) on templated carbon: This preparation follows that of Xaio and coworkers. A solution of $Cu(NO_3)_2 \cdot 2.5H_2O$ (0.024 g), $Ni(NO_3)_2 \cdot 6H_2O$ (0.016) in EtOH (1.01 g) was prepared and a zeolite templated carbon support (50 mg) was added to make a slurry. The slurry was stirred for 24 hrs, then sonicated for 2.5 hrs. The mixture was allowed to age for 3 days. The EtOH and water were removed on a rotovap at 80 °C and the dark black solid dried under vacuum for over night. The powder was calcined at 500 °C under nitrogen for 3 hrs and reduced at 600 °C under a stream of $5\%H_2/95\%\ N_2$. The powder X-ray diffraction showed the presence of nanoparticles of Cu and Ni.

Preparation of nano(Cu-Ni) on Norit A Supra carbon graphite: The carbon support was dried under vacuum for 24 hrs at 125 – 150 °C. The graphite was treated with solution of H_2SO_4:$KMnO_4$ at a ratio of C:H_2SO_4:$KMnO_4$ = 2.1g:12.6g:0.42g at 0 °C an additional 2 g of sulfuric acid was added to facilitate stirring (caution this is an extremely violent reaction). The reaction was allowed to stir overnight. The mixture was then heated at 40 – 50 °C for 2 hrs. The mixture was cooled to 0 °C and quenched with deionized water. The mixture was filtered and washed with water until the wash water had a pH of ~6. The mixture was air dried for 3 days, then dried at ~145 °C for 20 hrs under vacuum. The black graphite oxide was transferred to a vial and sealed. Although this type of graphite is not the same as the natural graphite and may not need this heating step it was subjected to it anyway in order to be consistent with the original literature procedure.

A tube furnace was set-up <u>in a good flowing hood</u> and heated to 900 °C with an argon flow. The graphite oxide (38 mg) was loaded into a crucible and pushed into the hot zone and held there for a few minutes. CAUTION this step produces CARBON MONOXIDE. The “thermally expanded” graphite is collected once cooled.

A solution of $Cu(NO_3)_2 \cdot 2.5H_2O$ (0.098 g), $Ni(NO_3)_2 \cdot 6H_2O$ (0.065) in EtOH (4.0 g)/H_2O (0.40 g) was prepared then added to the graphite oxide support (0.20 g) to make a slurry. The slurry was stirred for 40 hrs, then sonicated for 2 hrs. The mixture was allowed to age for 1 day. The EtOH and water were removed on a rotovap at 80 °C and the dark black solid dried under vacuum for 36 hrs at 90 °C. The powder was calcined at 500 °C (ramp rate = 5 °C/min) under nitrogen for 3 hrs and reduced at 600 °C (ramp rate = 5 °C/min) under a stream of $5\%H_2/95\%\ N_2$. The powder X-ray diffraction showed the presence of nanoparticles of Cu and Ni.

Preparation of nano(Cu-Ni) on natural flake graphite: The natural flake graphite (Alfa-Aesar, ~10 mesh,99.9% purity, Lot No. K285028) was dried under vacuum for 24 hrs at 120 °C. To the graphite (2.0 g) was added H_2SO_4 (3.5 g) then treated with solution of H_2SO_4:$KMnO_4$ at a ratio of C:H_2SO_4:$KMnO_4$ = 2.0g:12.0g:0.42g at 0 °C . The oxidation of the natural flake graphite is not as violent as that of the powdered graphite. The reaction was heated to 50 °C and stirred overnight. The mixture was centrifuged to remove the oxidizing solution. The mixture was washed with water on a filter membrane until the wash water had a pH of ~6 (many washings). The mixture was air dried vacuum dried overnight at 100 °C. The black graphite oxide was transferred to a vial and sealed.

A tube furnace was set-up in a good flowing hood and heated to 900 °C with an argon flow. The graphite oxide (0.46 g) was loaded into a crucible and pushed into the hot zone and held there for a few minutes. There was no evidence for carbon monoxide during this procedure. The natural flake graphite oxide (NFGO) expands tremendously during this stage. The NFGO was stirred with 200 mL of a 0.1 Molar NaOH/H_2O solution for 30 mins. It was then filtered over a membrane filter and washed two times with deionized water to a pH of 7 and air dried for ~30 mins.

To the NFGO (0.30 g) was added a mix a solution of $Cu(NO_3)_2$•$2.5H_2O$ (0.147 g), $Ni(NO_3)_2$•$6H_2O$ (0.098) in EtOH (6.0 g)/H_2O (0.60 g) and the slurry stirred for 24 hrs, then sonicated for 2 hrs. The mixture was allowed to age for 2 days. The EtOH was removed on a rotovap at 80 °C and the shiny curly solid dried under vacuum for 24 hrs at 90 °C. The powder was calcined at 500 °C (ramp rate = 5 °C/min) under nitrogen for 3 hrs and reduced at 600 °C (ramp rate = 5 °C/min) under a stream of 5%H_2/95% N_2. The powder X-ray diffraction showed the presence of nanoparticles of Cu and Ni.

3.2.4 Tin(II) Silyl amide Complexes

Synthesis of $Sn_4(\mu_4\text{-}O)(\mu_2\text{-}OSiMe_3)_5(\eta^1\text{-}N{=}C{=}S)$: Under argon, a Fisher Porter tube (fitted with a 120 psig pressure relief valve for safety) was loaded with $[(Me_3Si)_2N]_2Sn$ (1.440 g; 3.28 mmol) and dissolved in hexanes (2 g). To this system was attached a 74 cc stainless steel bomb. The solution was cooled to -100 ˚C and evacuated to remove the argon. The bomb was charged with 60 psig of OCS which was then condensed into the cooled $[(Me_3Si)_2N]_2Sn$/hexanes solution. This was repeated once more with 60 psig and then 20 psig to give a total of 140 psig of OCS (30.3 mmol). The reaction mixture was allowed to stir and slowly warm to 25 ˚C where it changed color from orange to yellow. The reaction was allowed to stir overnight at room temperature to eventually give a dark brown, cloudy solution. This solution was cooled to -78 ˚C and the excess OCS was removed under vacuum (alternatively the OCS can be removed under a stream of argon). The crude product obtained consisted of a black oil and solids (in some reactions a tin mirror was deposited on the sides of the glass vessel). The crude product was filtered and washed with pentane to give a black powder (0.150 g, Sn metal). From the pentane washings colorless crystals of $Sn_4(\mu_4\text{-}O)(\mu_2\text{-}OSiMe_3)_5(\eta^1\text{-}N{=}C{=}S)$ were obtained (0.310 g; 39% based on Sn; mp 192-193 ˚C dec.; slight color change to tan at 160 ˚C). The

volatiles were removed from the filtrate under an argon purge and analyzed by GC-MS. The by-products were found to be the following: $Me_3SiOSiMe_3$; $(Me_3Si)_2NH$; $Me_3SiN{=}C{=}S$; $Me_3SiN(H)C(S)OSiMe_3$; $Me_3SiN{=}C{=}NSiMe_3$. The by-products were not quantified. ^{1}H NMR (250 MHz, $CDCl_3$) δ 2.02 (s, C*H*$_3$) ppm. ^{13}C{^{1}H} NMR (62 MHz, $CDCl_3$) δ 176.52 (O-*C*-S), 3.63 (*C*H$_3$) ppm. ^{119}Sn{^{1}H} (93.27 MHz, $CDCl_3$, ref. to Me_4Sn) δ 108-107 (broad mult), -143 (s) ppm. IR (Nujol): ν = 2044 (s), 1263 (s), 1249 (s), 871 (s), 838 (s), 751 (s) cm^{-1}.

Bis(2,2,5,5-tetramethyl-1-aza-2,5-disilacyclopent-1-yl)tin: Procedures similar to those reported by Wrackmeyer[39] and Westerhauser[40] were followed. Under argon 2,2,5,5-tetramethyl-2,5-disilyl-1-aza-cyclopentane (6.0 g, 37.6.0 mmol) was dissolved in 50 mL of diethyl ether then cooled to 0 °C. *n*-Butyllithium (2.5 *M* in hexanes, 15.0 ml, 37.6 mmol) was added drop-wise and the mixture was allowed to warm to room temperature over a two hour period with stirring. The resulting solution was added drop-wise through a cannula to a solution of tin dichloride (3.58 g, 19.0 mmol) in 50 mL mixture of THF/Et_2O held at 0 °C. The reaction mixture was allowed to warm to room temperature while stirring overnight. The lithium chloride precipitate was filtered using a glass frit and Celite as a filtering aid. The solvent was removed from the filtrate at reduced pressure and the crude product distilled at reduced pressure (45 μHg). The product was collected between 87 - 100 °C as a red oil. Yield: 5.18 g (63%). ^{1}H NMR (250 MHz, C_6D_6) δ 0.76 (s, 4H, C*H*$_2$), 0.18 (s, 6H, C*H*$_3$) ppm. ^{13}C{^{1}H} NMR (63 MHz, C_6D_6) δ 11.57 (s, *C*H$_2$), 4.04 (s, *C*H$_3$) ppm. ^{119}Sn{^{1}H} (93.27 MHz, C_6D_6) δ 808 (Lit. δ = 798[39] or 821[40]) ppm.

Reaction of bis(2,2,5,5-tetramethyl-1-aza-2,5-disilacyclopent-1-yl)tin with CO_2 to give $Sn_4(\mu_4\text{-}O)(\mu_2\text{-}O_2C[tmdacp]_4)(\mu_2\text{-}N{=}C{=}O)_2$: In an argon-purged Fisher Porter reactor tube, bis(2,2,5,5-tetramethyl-1-aza-2,5-disilacyclopent-1-yl)tin (0.20 g, 0.45 mmol) was dissolved in 20 mL anhydrous pentane at room temperature. The bottle was charged with CO_2 (60 psig) and allowed to react for approximately an hour. The solvent was removed at reduced pressure and the crude product was extracted with toluene, filtered and cooled to –20 °C. After several days at low temperature yellow crystals were obtained. The crystals were isolated and identified as $Sn_4(\mu_4\text{-}O)(\mu_2\text{-}O_2C[N(SiMe_2(CH_2)_2)]_4)(\mu_2\text{-}N{=}C{=}O)_2$ (**2**) (0.08 g, yield 50% based on tin, mp 102-104 °C). ^{1}H NMR (250 MHz, C_6D_6) δ 0.71 (s, 16H, C*H*$_2$), 0.40 (s, 24H, Si(C*H*$_3$)$_2$) ppm. ^{13}C{^{1}H} NMR (63 MHz, C_6D_6) δ 180.5 (N=*C*=O), 167.9 (*C*O$_2$), 8.4 (C*H*$_2$), -0.4 (C*H*$_3$) ppm. ^{119}Sn{^{1}H} (93 MHz) δ -316 ppm. Anal. Calcd for $C_{30}H_{64}N_6O_{11}Si_8Sn_4$ (M_w = 1384.26): C, 25.95; H, 4.66 N; 4.04. Found: C, 25.82; H, 4.62; N, 3.98. The predominant by-product from the mother liquors was 2,2,5,5-tetramethyl-2,5-disila-tetrahydrofuran and was identified by GC-MS. (Calcd for $C_6H_{16}OSi_2$, 160.4). GC-MS *m/z* (relative intensity, ion): 160 (16%, M^+), 145 (100%, M^+ - CH_3), 117 (100%, $Me_3SiO(CH_2)_2^+$), 73 (90%, $CH_3SiOCH_2^+$).

Reaction of bis(2,2,5,5-tetramethyl-1-aza-2,5-disilacyclopent-1-yl)tin with COS: Under an argon atmosphere, a solution of bis(2,2,5,5-tetramethyl-1-aza-2,5-disilacyclopent-1-yl)tin (0.54 g, 1.2 mmol) and petroleum ether (3 g) was cooled to -78 °C and then evacuated to remove the argon. At -78 °C carbonyl sulfide (2.4 mmol) was

condensed into the reaction vessel. As the reaction warmed to room temperature a red-brown precipitate formed. The precipitate was filtered from solution and washed several times with petroleum ether. Upon drying 0.153 g of a rust-colored solid was collected. This solid was insoluble in the following solvents: petroleum ether, pentane, diethyl ether, THF, methylene chloride, acetonitrile, toluene, and pyridine. The insolubility of this compound precluded characterization. However, the IR and elemental analyses are reported. IR (Nujol): ν = 2277 (m), 2066 (s), 1972 (m), 1255 (m) 1054 (m), 794 (m) cm^{-1}. Elemental analysis of C, H, N, S, and Sn gave: C, 11.92; H, 1.74; N, 6.48; S, 17.7; Sn, 52.4. The GC-MS of the filtrate indicated petroleum ether and 2,2,5,5-tetramethyl-2,5-disila-tetrahydrofuran (Calcd for $C_6H_{16}OSi_2$, 160.4). (GC-MS *m/z* (relative intensity, ion) 160 (10%, M^+), 145 (100%, $M^+ - CH_3$).

Reaction of bis(2,2,5,5-tetramethyl-1-aza-2,5-disilacyclopent-1-yl)tin with CS_2 to give $\{[tmdacp]_2Sn\}_2CS_2$---$\{Sn(tmdacp)_2\}$: To a solution of bis(2,2,5,5-tetramethyl-1-aza-2,5-disilacyclopent-1-yl)tin (1.50 g, 3.44 mmol) in hexane (7 g) held at room temperature, CS_2 (1.0 mL, 13.1 mmol) was added drop-wise. The reaction was immediate with the color changing from red-orange to dark green. The reaction was allowed to stir for 1 hour. Volatiles were removed until crystallization began to occur. The dark green solution was cooled to –20 °C overnight. Green crystals of $\{[tmdacp]_2Sn\}_2CS_2$---$\{Sn(tmdacp)_2\}$ were obtained (1.59 g, yield 99 %, mp 98 °C). ^1H NMR (250 MHz, C_6D_6) δ 0.83 (s, 16 H, C*H*$_2$), 0.30 (s, 24 H, Si(C*H*$_3$)$_2$) ppm. $^{13}C\{^1H\}$ NMR (63 MHz, C_6D_6) δ 11.4 (s, CH_2), 3.9 (s, CH_3), S=*C*=S not observed. $^{119}Sn\{^1H\}$ (93.27 MHz, C_6D_6) δ 363 (broad), 83.5 (s), 18.0 (s) ppm. IR (Nujol): ν = 1523 (w), 869 (s).

3.2.5 Group 2 silyl amides

$Mg(tmdacp)_2(Et_2O)_2$: *n*-BuLi (15.0 mL, 37.5 mmol, 2.5 M in hexanes) was added dropwise to a solution of tmdacp (5.78 g, 36.3 mmol) in 100 mL of diethyl ether and the reaction mixture was stirred for 2 hours. Subsequently, $MgBr_2$ (3.33 g, 18.1 mmol) was gradually added to the mixture and stirred for 12 hours. Solvent was removed under vacuum and the residue was suspended in toluene. The mixture was filtered to remove LiBr. Crystals of $Mg\{c\text{-}N[Si(CH_3)_2CH_2]_2\}_2(Et_2O)_2$ were obtained from toluene at -20 °C. Yield 76% (0.67 g), m.p. 85 °C (loss of solvent), 100 °C (dec.). ^1H NMR (250 MHz, THF-d_8): δ 0.00 (s, 24H, Si(C*H*$_3$)$_2$CH$_2$), 0.49 (s, 8H, Si(CH$_3$)$_2$C*H*$_2$), 1.21 (m, 4H, O(CH$_2$C*H*$_3$)$_2$), 3.50 (m, 6H, O(C*H*$_2$CH$_3$)$_2$). $^{13}C\{^1H\}$ (63 MHz, THF-d_8): δ 4.85 (Si(*C*H$_3$)$_2$CH$_2$), 12.62 (Si(CH$_3$)$_2$*C*H$_2$), 15.35 (O(CH$_2$*C*H$_3$)$_2$), 65.97 (O(*C*H$_2$CH$_3$)$_2$).

Reaction of $Mg(Tmdacp)_2(Et_2O)_2$ with CO_2: A 5 mm uncapped NMR tube containing $Mg(tmdacp)_2(Et_2O)_2$ (0.397 g, 0.80 mmol) was placed inside a stainless-steel, high-pressure reactor. The reactor was then pressurized with CO_2 to 700 psig and allowed to interact in a solid/gas reaction for 5 hours. The reaction vessel was then carefully degassed. IR spectroscopy of the resulting solid showed: ν_{max} cm^{-1} (Nujol) 1614 s (asym -C-O), 1529 s (sym -C-O). This product was dissolved in 8 mL pyridine. Crystals formed after 8 hours and were characterized by X-ray diffraction as $Mg(NCO)_2(py)_5$. Yield 0.172

g (98.6% based on Mg), m.p. 210-212 °C (loss of solvent), >300 °C (did not decompose). ν_{max} cm^{-1} (Nujol) 2227 s (asym -N=C=O), 2199 s (asym -N=C=O).

3.2.6 Phosphino amide ligands and their Group 2 and 12 complexes

HN(*i*-$Pr_2P)_2$ and HN(*i*-Pr_2P)($SiMe_3$): A solution of chlorodiisopropylphosphine (15.0 g, 98 mmol) in 20 mL anhydrous toluene was added dropwise to a solution of hexamethyldisilazane in 40 mL toluene. The colorless solution was allowed to stir overnight, then the solvent and chlorotrimethylsilane were removed under vacuum. HN(*i*-Pr_2P)($SiMe_3$) was separated by vacuum distillation (20 μm Hg, 27-32 °C), leaving HN(*i*-$Pr_2P)_2$ that was recrystallized from pentane. Yield **HN(*i*-Pr_2P)($SiMe_3$)** = 8.45 g. ^{1}H NMR (250 MHz, C_6D_6): δ 0.17 (s, 9H, $SiMe_3$), 0.88-1.04 (overlapping doublets, 12H, PCH(C*H*$_3)_2$), 1.33 (sept, 2H, PC*H*$(CH_3)_2$). $^{31}P\{^1H\}$ NMR (101 MHz, C_6D_6): δ 48.7. Yield **HN(*i*-$Pr_2P)_2$** = 5.75 g. ^{1}H NMR (250 MHz, C_6D_6): δ 0.99-1.09 (overlapping doublets, 24H, PCH(C*H*$_3)_2$), 1.47 (sept, 4 H, PC*H*$(CH_3)_2$). $^{31}P\{^1H\}$ NMR (101 MHz, C_6D_6): δ 68.0. HN(*i*-$Pr_2P)_2$ can be prepared in higher yields by using a 2:1 ratio of chlorodiisopropylphosphine and hexamethyldisilazane under the same reaction conditions.

Mg[N(*i*-Pr_2P)($SiMe_3$)]$_2$(THF): Dibutylmagnesium (2.4 mL, 2.4 mmol, 1.0 M in heptane) was added dropwise to a solution of HN(*i*-Pr_2P)($SiMe_3$) (1.00 g, 4.9 mmol) in ca. 10 mL anyhydrous THF. The colorless solution was allowed to stir for 3 hours, and then the solvent was removed under vacuum. The residue was dissolved in pentane and cooled to -25 °C. After one week, colorless crystals of Mg[N(*i*-Pr_2P)($SiMe_3$)]$_2$(THF) were isolated. Yield = 0.577 g (47%). $^{31}P\{1H\}$ NMR (101 MHz, THF): δ 73.5 ppm.
M[N(*i*-Pr_2P)($SiMe_3$)]$_2$(THF)$_2$ (M = Ca or Sr): Potassium hydride (0.29 g, 7.30 mmol) was added to a solution of HN(*i*-Pr_2P)($SiMe_3$) (1.00 g, 4.9 mmol) in ca. 15 mL anhydrous THF. After overnight stirring, the excess KH was removed by filtration and the pale yellow solution of KN(*i*-Pr_2P)($SiMe_3$) was added to a suspension of CaI_2 or SrI_2 (2.4 mmol) in ca. 15 mL anhydrous THF. The cloudy white mixture was allowed to stir for three hours, and then solvent was removed under vacuum. The residue was suspended in ca. 20 mL toluene and filtered to remove KI. Toluene was removed under vacuum and the residue was dissolved in minimal pentane. Cooling to -25 °C overnight gave large, block-like colorless crystals that were characterized by X-ray diffraction. **Ca[N(*i*-Pr_2P)($SiMe_3$)]$_2$(THF)$_2$:** ^{1}H NMR (250 MHz, C_6D_6): δ 0.43 (s, 18H, Si(C*H*$_3)_3$), 1.16-1.38 (overlapping doublets, 32H, PCH(C*H*$_3)_2$ and THF), 1.99 (sept, 4H, PC*H*$(CH_3)_2$), 3.65 (m, 8H, THF). $^{31}P\{1H\}$ NMR (101 MHz, C_6D_6): δ 67.7. **Sr[N(*i*-Pr_2P)($SiMe_3$)]$_2$(THF)$_2$:** ^{1}H NMR (250 MHz, C_6D_6): δ 0.42 (s, 18H, Si(C*H*$_3)_3$), 1.15-1.37 (overlapping doublets, 32H, PCH(C*H*$_3)_2$ and THF), 1.96 (sept, 4H, PC*H*$(CH_3)_2$), 3.59 (m, 8H, THF). $^{31}P\{1H\}$ NMR (101 MHz, C_6D_6): δ 68.1.

{EtZn[N(*i*-Pr_2P)($SiMe_3$)]}$_2$: Diethylzinc (5.3 mL, 5.3 mmol, 1.0 M in hexanes) was added dropwise to a solution of HN(*i*-Pr_2P)($SiMe_3$) (1.00 g, 4.9 mmol) in ca. 10 mL anhydrous THF. The colorless solution was allowed to stir for 3 hours, then the volatiles were removed under vacuum. The residue was dissolved in minimal pentane and cooled

to -25 °C. After one week, large, rod-shaped, colorless crystals that were characterized by X-ray diffraction as $\{EtZn[N(i\text{-}Pr_2P)(SiMe_3)]\}_2$ were isolated. Yield = 0.91 g (63%). ^{1}H NMR (250 MHz, C_6D_6): δ 0.28 (s, 9H, $Si(CH_3)_3$), 0.55 (q, J = 8 Hz, 2H, $ZnCH_2CH_3$), 0.94-1.16 (overlapping doublets, 12H, $-PCH(CH_3)_2$), 1.53 (t, J = 8 Hz, 3H, $ZnCH_2CH_3$), 1.92 (sept, 2H, $-PCH(CH_3)_2$). ^{31}P{1H} NMR (101 MHz, THF): δ 60.3.

$M[N(PPh_2)_2]_2(THF)_3$ (M = Ca or Sr): Prepared according to a variation of literature procedures.[31,32] Potassium hydride (0.21 g, 5.2 mmol) was added slowly to a solution of $HN(PPh_2)_2$ (2.00 g, 5.2 mmol) in ca. 15 mL anhydrous THF. When evolution of H_2 gas had ceased, the solution was added dropwise to a suspension of CaI_2 or SrI_2 (2.6 mmol) in ca. 15 mL anhydrous THF. The cloudy mixture was allowed to stir for 3 hrs, then solvent was removed under vacuum. The residue was suspended in ca. 20 mL toluene and filtered to remove KI. The toluene was removed under vacuum and the crude product was recrystallized at -25 °C from a 1:1 mixture of THF and pentane.

$\{EtZn[N(PPh_2)_2]\}_2$: Diethyl zinc (5.2 mL, 5.2 mmol, 1 M in hexanes) was added dropwise to a suspension of $HN(PPh_2)_2$ (2.00 g, 5.2 mmol) in ca. 25 mL anhydrous THF. The mixture was allowed to stir for 1 hour, during which time it became a clear, colorless solution. Volatiles were removed under vacuum and the residue was dissolved in a 2:1 mixture of THF and pentane. Cooling to -25 °C overnight gave colorless crystals that were characterized by X-ray diffraction. Yield = 2.19 g (88%), mp = 136 °C (dec). ^{31}P{^{1}H} NMR (101 MHz, THF-d_8): δ 49.0.

Reaction of $M[N(PPh_2)_2]_2(THF)_3$ (M = Ca or Sr) with CO_2: Carbon dioxide was bubbled into a colorless solution of $M[N(PPh_2)_2]_2(THF)_3$ (0.75 g) in ca. 10 mL anhydrous THF. After 15 minutes, the solution was purged with argon and left undisturbed at room temperature. Colorless, needle-like crystals (Sr) or white precipitate (Ca) formed over a period of weeks and were isolated by decanting the solvent. **Sr complex:** Yield = 0.067 g (15% based on Sr). Mp = 177-178 °C. Elem. Anal for $C_{184}H_{176}N_8O_{31}P_{12}Sr_6$: Calcd: C, 56.77; H, 4.56; N, 2.88. Found: C, 56.95; H, 4.50; N, 2.88. IR (cm^{-1}): ν = 1659 (vs), 1620(s) 1604 (s). CP-MAS ^{31}P NMR (101 MHz): δ = 36.5 ppm. By-products including $Ph_2P\text{-}Ph_2P{=}N\text{-}PPh_2$, $N(PPh_2)_3$ and $HN(PPh_2)_2$ were identified by ^{31}P NMR spectra of the crude reaction mixture, but were not isolated. **Ca complex:** Yield = 0.117 g (30% based on Ca). Elem. Anal for $C_{184}H_{176}N_8O_{31}P_{12}Ca_6$: Calcd: C, 61.26; H, 4.92; N, 3.11. Found: C, 61.57; H, 5.96; N, 2.53 IR (cm^{-1}): ν = 1668 (vs), 1624 (s), 1606 (s). CP-MAS ^{31}P NMR (101 MHz): δ = 35.7.

Reaction of $M[N(i\text{-}Pr_2P)(SiMe_3)]_2(THF)_x$ (M = Mg, x = 1; M = Ca or Sr, x = 2) with CO_2: Carbon dioxide was bubbled into a colorless solution of $M[N(i\text{-}Pr_2P)(SiMe_3)]_2(THF)_x$ (100 mg) in ca. 10 mL hexanes. After 15-20 minutes, the solution was purged with argon and analyzed. IR (cm^{-1}): ν = 2257 (vs), 1586 (s). ^{31}P{^{1}H} NMR (101 MHz, C_6H_{14}): δ 89.4. GC-MS (M/Z): 159 ($i\text{-}Pr_2PN{=}C{=}O$), 117 ($i\text{-}Pr_2P$). The metal-containing product, $[M(OSiMe_3)_2]_n$ was not isolated.

Reaction of $\{EtZn[N(i\text{-}Pr_2P)(SiMe_3)]\}_2$ with CO_2: Carbon dioxide was bubbled into a colorless solution of $\{EtZn[N(i\text{-}Pr_2P)(SiMe_3)]\}_2$ (0.39 g) in ca. 10 mL hexanes. After 15 minutes, the solution was purged with argon and left undisturbed at room temperature. Over the course of several days, two distinct colorless crystals were formed in the solution. The block-shaped and rod-shaped crystals were separately characterized by X-ray crystallography and found to be $C_{20}H_{46}N_2O_4P_2Si_2Zn$ and $C_{78}H_{178}N_6O_{10}Si_4P_8Zn_6$, respectively.

Reaction of $Mg[N(i\text{-}Pr_2P)(SiMe_3)]_2(THF)$ with CS_2: Carbon disulfide (0.034 mL, 0.56 mmol) was added dropwise to a solution of $Mg[N(i\text{-}Pr_2P)(SiMe_3)]_2(THF)$ (0.14 g, 0.28 mmol) in 10 mL anhydrous pentane. An immediate color change to deep green was observed. The reaction was allowed to stir for 15 minutes, and was then concentrated under vacuum until a white precipitate began to form. The green supernatant solution was decanted and cooled to -25 °C overnight to yield green crystals that were characterized by X-ray diffraction as $Mg\{N[i\text{-}Pr_2P(=S)](SiMe_3)\}_2(THF)$. $^{31}P\{^1H\}$ NMR (101 MHz, THF): δ 78.0. Characterization of the white precipitate is underway.

Reaction of $Ca[N(i\text{-}Pr_2P)(SiMe_3)]_2(THF)_2$ with CS_2: Same as above, beginning with 0.20 g (0.34 mmol) of the calcium complex. Upon addition of CS_2, the mixture immediately turned amber and a yellow precipitate formed within seconds. Colourless to pale yellow crystals that were obtained after cooling the decanted supernatant overnight were characterized by X-ray diffraction as $Ca\{N[i\text{-}Pr_2P(=S)](SiMe_3)\}_2(THF)$. Characterization of the yellow precipitate is underway.

Reaction of $M[N(PPh_2)_2]_2(THF)_3$ (M = Ca, Sr) with CS_2: Carbon disulfide (2 eq) was added dropwise to a solution of $Sr[N(PPh_2)_2]_2(THF)_3$ (1.00 g, 0.93 mmol) or $Ca[N(PPh_2)_2]_2(THF)_3$ (0.75 g, 0.73 mmol) in ca. 40 mL anhydrous THF. An immediate color change to bright red was observed. After stirring for 15 minutes, the solution was concentrated under vacuum to a volume of ca. 10 mL and cooled to -25 °C. Yellow crystals (Sr) or orange precipitate (Ca) grew out over several days and were isolated by decanting the red supernatant solution. The crystals were characterized by X-ray diffraction as $Sr\{N[P(=S)Ph_2]_2\}_2(THF)_2$. $^{31}P\{^1H\}$ NMR (101 MHz, THF): δ 38.0 (Sr), 37.1 (Ca).

Reaction of $\{EtZn[N(PPh_2)_2]\}_2$ with CS_2: Carbon disulfide (4 eq.) was added to a solution of $\{EtZn[N(PPh_2)_2]\}_2$ that had been prepared *in situ* as described above. An immediate color change to red-orange was observed, and a yellow-orange precipitate formed with 5 minutes. The reaction mixture was allowed to stir for 1 hour, and then the solution and precipitate were separated by filtration. Cooling the supernatant to -25 °C for several weeks yielded red crystals that were characterized by X-ray diffraction as $Zn\{N[P(=S)Ph_2]_2\}_2$. $^{31}P\{^1H\}$ NMR (101 MHz, THF): δ 38.1.

Reaction of $HN(PPh_2)_2$ with CS_2: Carbon disulfide (0.16 mL, 2.59 mmol) was added to a solution of $HN(PPh_2)_2$ (1.00 g, 2.59 mmol) in ca. 30 mL anhydrous THF. Over the course of 15 minutes, the solution developed a deep red color. The solvent was removed after stirring for 45 minutes, and the purple-brown residue was suspended in toluene. After filtration to remove an insoluble white precipitate, the yellow supernatant was cooled to -25 °C. Colorless crystals were isolated after several days and characterized by X-ray diffraction as $[Ph_2P(=S)N=P(Ph)_2S]_2$.

Reaction of $HN(i\text{-}Pr_2P)(SiMe_3)$ with CS_2: Carbon disulfide (0.35 mL, 5.84 mmol) was added to a solution of $HN(i\text{-}Pr_2P)(SiMe_3)$ (1.00 g, 4.87 mmol) in ca. 15 mL anhydrous pentane. The solution quickly developed an intense red color. After 1 hour, the solvent was removed and the residue was recrystallized from minimal anhydrous THF at -25 °C to give large red, plate-like crystals characterized by X-ray diffraction as $HN[i\text{-}Pr_2P(CS_2)](SiMe_3)$. $^{31}P\{^1H\}$ NMR (101 MHz, C_6D_6): δ 33.7.

Reaction of $HN(i\text{-}Pr_2P)_2$ with CS_2: Carbon disulfide (0.2 mL, 3.3 mmol) was added to a solution of $HN(i\text{-}Pr_2P)_2$ (0.83 g, 3.3 mmol) in ca. 15 mL anhydrous THF. An immediate color change to dark red was observed. After one hour, the volume of the solution was reduced under vacuum to ca. 5 mL and then was cooled to -25 °C. Red-orange rod-shaped crystals were isolated after several hours and characterized by X-ray diffraction as $(i\text{-}Pr_2PH)N=[P(i\text{-}Pr)_2(CS_2)]$. ^1H NMR (250 MHz, C_6D_6): δ 0.72 (d, $^3J_{HH}$ = Hz, 6H, $PCH(CH_3)_2$), 0.79 (d, $^3J_{HH}$ = 7 Hz, 6H, $PCH(CH_3)_2$), 0.98 (d, $^3J_{HH}$ = 7 Hz, 3H, $PCH(CH_3)_2$), 1.04 (d, $^3J_{HH}$ = 7 Hz, 3H, $PCH(CH_3)_2$), 1.16 (d, $^3J_{HH}$ = 7 Hz, 3H, $PCH(CH_3)_2$), 1.22 (d, $^3J_{HH}$ = 7 Hz, 3H, $PCH(CH_3)_2$), 1.88 (m, 2H, $PCH(CH_3)_2$), 2.60 (m, 2H, $PCH(CH_3)_2$), 7.24 (d, $^1J_{PH}$ = 480 Hz, P*H*). $^{31}P\{^1H\}$ NMR (101 MHz, C_6D_6): δ 33.9 (d, $^2J_{PP}$ = 33 Hz, $^1J_{PH}$ = 480 Hz), 35.1 (d, $^2J_{PP}$ = 33 Hz).

Table 3.2.1 List of cyclams and characterization data.

Cyclam	^{1}H NMR	^{13}C NMR	IR	X-ray	Preparation ref.
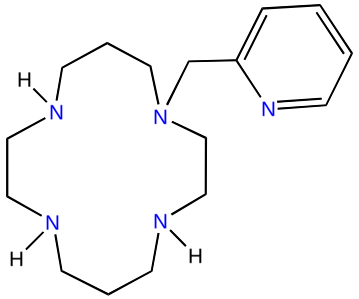			Neat – KBr plate 3292, m 2927, m; 2877, m; 2807, s 1670, w 1589, m 1569, w 1471, s; 1434, m 1121, s 1070, w 753, s 638, w; 615, w	yes	I. Meunier, A. K. Mishra, B. Hanquet, P. Cocolios and R. Guilard, *Can. J. Chem.* 1995, **73**, 685-695.
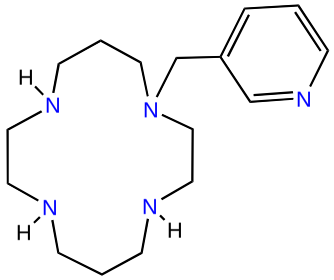			Neat – KBr plate 3272, s; 3187, m 2925, s; 2881, s; 2808, vs 1668, m 1577,w 1463, s; 1425, m 1336, w 1279, w 1221, w;1120, s;1074, w 791, s; 748, m; 714, s 653, w; 617, w	yes	I. Meunier, A. K. Mishra, B. Hanquet, P. Cocolios and R. Guilard, *Can. J. Chem.* 1995, **73**, 685-695.
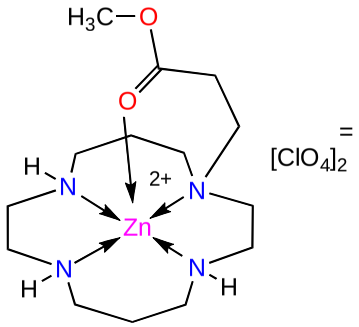			Nujol 3318, w; 3293, w 2196, w; 2063, w 1651, m 1384, m 1308, w 1082, s 931, w	yes	This work.

	^{1}H NMR	^{13}C NMR	IR	X-ray	ref
Cyclam 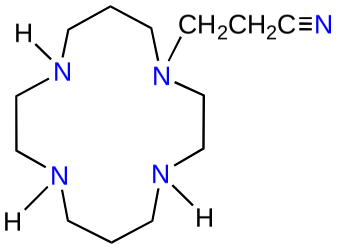	($CDCl_3$) 3.34, broad s/3.26, s 6 H 2.5, mult., 20 H 1.6, mult., 3.6 H 0.93, d, 0.5 H		Neat – KBr plate 3286, s 2922, s 2819, s 2247, s (CN) 1660, m (CN) 1558, m 1464, s 1349, s 1278, s; 1132, s 1042, m 753, s; 658, w	yes	H. Fensterbank, J. Zhu, D. Riou and C. Larpent, *J. Chem. Soc., Perkins Trans. 1*, 1999, 811-815. K. Q. Ferreira, F. G. Doro and E. Tfouni, *Inorg, Chim. Acta*, 2003, **355**, 205-212.
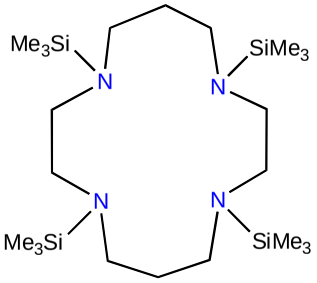	($CDCl_3$) 2.86, mult. 12.8 H 1.8, mult., 2.8 H 0.31, s, 36 H	($CDCl_3$) 47.9 46.2 30.3 -0.14	Nujol 2073, w 1681, w 1339, w 1166, s 1119, m; 1047 s 987, s/m 834, br s 745, s 677, m	yes	This work.
CAS-9-72 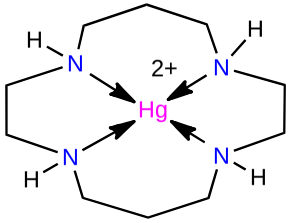 = $[ClO_4]_2$				yes	This work.

Cyclam	^{1}H NMR	^{13}C NMR	IR	X-ray	Ref
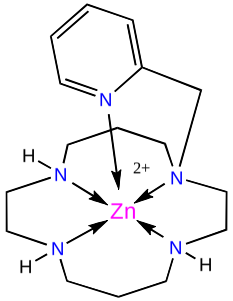 = $[ClO_4]_2$	8.70, m, 1 H 8.20, m, 1 H 7.70, m, 2 H 4.49, d, J_{HH} = 16.5 Hz, 0.5 H 3.89, d, J_{HH} = 16.7 Hz, 0.5 H 3.00, m, 12 H 1.28, m, 3.4 H	too insoluble	Nujol 3585, m 3271, m 3241, m 2023, w 1651, m 1612, s 1067, s 804, m 714, m 623, s	yes	This work
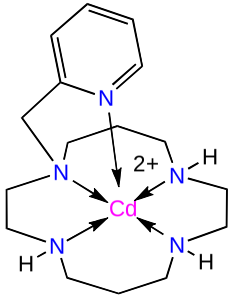	8.70, m, 1.6 H 8.00, m, 1.6 H 7.54, m, 3.9 H 4.31, d, J_{HH} = 15.6 Hz, 1 H 3.71, d, J_{HH} = 16.0 Hz, 1.5 H 2.93, m, 23.6 H 2.48, m, 0.8 H 1.79, m, 5.4 H	too insoluble	Nujol 3263, w 2217,w 1610, w 1299, vw 1082, s 1024, m 769, m 623, m	yes	This work
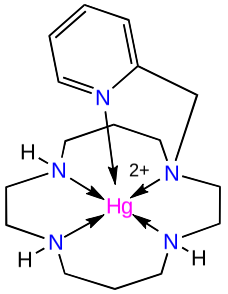 = $[ClO_4]_2$	8.66, m, 1.3H 8.07, m, 1.0 H 7.65, m, 3.24 H 4.32, d, J_{HH} = 15.8 Hz, 1 H 3.73, d, J_{HH} = 16.0 Hz, 1 H 2.94, m, 18.4 H 1.88, m, 4.4 H	too insoluble	Nujol 3269, w 1291, w 1080, s 1017, m 720, w 622, s 428, m		This work

4 SUMMARY AND CONCLUSIONS

A new catalyst, di-*n*-octyl dimethoxy tin, was prepared and its activity tested in the production of dimethyl carbonate (DMC) using CO_2 and methanol. The initial results appear to give superior results to that of di-*n*-butyl dimethoxy tin. However, the di-*n*-octyl tin catalyst was still susceptible to hydrolysis in spite of the more hydrophobic octyl groups attached to the tin. There is no simple way around the water issue when making DMC from methanol and carbon dioxide. This led us to investigate the viability of zinc cyclams as DMC catalysts.

Initially the zinc cyclam complexes showed good promise as potential catalysts for the synthesis of DMC from CO_2 and methanol. These complexes readily take up carbon dioxide in methanol at ambient temperatures and pressures to give the metal methyl carbonates and are stable to water. However numerous conditions from mild to extreme proved unsuccessful in introducing another molecule of methanol into the metal reaction sphere to form and then eliminate DMC. Modification of the macrocyclic ring via the attachment of various functionalized arms was undertaken in an effort at inducing additional reactivity at the metal center. This resulted in a number of new zinc and cadmium pyridinyl-substituted cyclam complexes that were structurally characterized. None of these new metal pyridinyl cyclam complexes proved effective at producing DMC. A collaboration with Prof. Rybak-Akimova at Tufts University, whose group is actively involved in the research of similar tetra- and pentaazamacrocyclic metal compounds, will be initiated to prepare and study new zinc complexes with pyridine containing macrocycles bearing pendant arms.

The reaction of CO_2 with $(tmdacp)_2Sn$ formed a novel tin-oxo cluster with the by-product of CO. This resulted in the splitting of CO_2 into oxygen and CO at room temperature and at low pressures. This result clearly warrants further investigation with the goal of understanding this mechanism of CO_2 activation and making this process catalytic.

The treatment of $(tmdacp)_2Sn$ with CS_2 also led to some very interesting chemistry. In this case one molecule of CS_2 complexed to three $(tmdacp)_2Sn$ molecules through the tin atoms ($\{[tmdacp]_2Sn\}_2CS_2$---$\{Sn(tmdacp)_2\}$). This complex, which is a dark green crystalline solid, was shown to be reversibly thermochromic in solution, going from dark green at room temperature to dark yellow at high temperature. In addition, this dark green complex reacts with carbon dioxide at room temperature in the solid state. Structural analysis of this complex has shown that the carbon sulfur bonds have elongated and the central carbon has re-hybridized. These observations suggest that this complex is a type of transition state showing activation of the carbon disulfide. This information could be useful in determining how to activate carbon dioxide. Tin Mössbauer spectroscopy is currently underway to determine the tin oxidation states of this unusual complex.

One of the goals of this work was to find routes to make useful, high-value chemicals using carbon dioxide. In the past Prof. Sita and coworkers reported the reaction of group 14 metal silyl amides (M = Ge, Sn) with CO_2 at room temperature to form isocyanates and carbodiimides over several hours.[22] By concentrating our efforts on the more electropositive group 2 metal silyl amides (M = Mg, Ca, Sr) we have been able to reduce the reaction time from hours to minutes to make isocyanates and carbodiimides. Work is still underway to make this process catalytic.

By replacing silicon with phosphorus to give phosphino-substituted amide group 2 metal complexes ($M[N(PPh_2)_2]_2$, M = Ca, Sr) the resulting chemistry with CO_2 was found to be completely different. Instead of producing isocyanates and carbodiimides with carbon dioxide these group 2 metal complexes gave M_6 clusters and in the process fixed 12 molecules of CO_2 into two, new types of ligands – a phosphino-substituted carbamate and a completely unknown $[N(CO_2)_3]^{3-}$ ligand. This was all accomplished at room temperature and atmospheric pressure. This remarkable and very important result demonstrates that our original concept of using electropositive metal ions to "fix" CO_2 is valid.

Reactions of these bis-(di-phosphino-amido) group 2 complexes with CS_2, although different from the CO_2 results, exhibited a rich and diverse chemistry as well. These group 2 complexes split CS_2 into S and "CS" with the sulfur oxidizing the phosphorus atoms the fate of the "CS" still unknown. Splitting or activation of CS_2 is known to occur with transition metals, but this is unprecedented for main-group elements.

5 REFERENCES

(1) Aresta, M.; Dibenedetto, A. *Dalton Trans.* **2007**, 2975-2992.
(2) Choi, J.-C.; Sakakura, T.; Sako, T. *J. Am. Chem. Soc.* **1999**, *121*, 3793-3794.
(3) Suciu, E. N.; Kuhlmann, B.; Knudsen, G. A.; Michaelson, R. C. *J. Organomet. Chem.* **1998**, *556*, 41-54.
(4) Ballivet-Tkatchenko, D.; Chermette, H.; Plasseraud, L.; Walter, O. *Dalton Trans.* **2006**, 5167-5175.
(5) Kohno, K.; Choi, J.-C.; Ohshima, Y.; Yili, A.; Yasuda, H.; Sakakura, T. *J. Organomet. Chem.* **2008**, *693*, 1389-1392.
(6) Ballivet-Tkatchenko, D.; Chambrey, S.; Keiski, R.; Ligabue, R.; Plasseraud, L.; Richard, P.; Turunen, H. *Catal. Today* **2006**, *115*, 80-87.
(7) Kato, M.; Ito, T. *Inorg. Chem.* **1985**, *24*, 509-514.
(8) Kato, M.; Ito, T. *Inorg. Chem.* **1985**, *24*, 504-508.
(9) Kato, M.; Ito, T. *Bull. Chem. Soc. Japan* **1986**, *59*, 285-294.
(10) Cai, Q.; Lu, B.; Guo, L.; Shan, Y. *Catal. Commun.* **2009**, *10*, 605-609.
(11) Meunier, I.; Mishra, A. K.; Hanquet, B.; Cocolios, P.; Guilard, R. *Can. J. Chem.* **1995**, *73*, 685-695.
(12) Ferreira, K. Q.; Doro, F. G.; Tfouni, E. *Inorg. Chim. Acta* **2003**, *355*, 205-212.
(13) Pinner, A.; Klein, F. *Chem. Ber.* **1877**, *10*, 1889.
(14) March, J. *Advanced Organic Chemistry: Reactions, Mechanisms and Structure*; 4th ed.; Wiley & Sons: New York, 1992.
(15) Bian, J.; Xiao, M.; Wang, S.; Wang, X.; Lu, Y.; Meng, Y. *Chem. Eng. J.* **2009**, *147*, 287-296.
(16) Bian, J.; Xiao, M.; Wang, S. J.; Lu, Y. X.; Meng, Y. Z. *J. Colloid Interface Sci.* **2009**.
(17) Tang, Y.; Felix, A. M.; Boro, B. J.; Zakharov, L. N.; Rheingold, A. L.; Kemp, R. A. *Polyhedron* **2005**, *24*, 1093-1100.
(18) Tang, Y.; Felix, A. M.; Manner, V. W.; Zakharov, L. N.; Rheingold, A. L.; Moasser, B.; Kemp, R. A. *Synthesis and Characterization of Divalent Main Group Diamides and Reactions with CO_2*; Oxford University Press: Washington, DC, 2006; Vol. 917.
(19) Tang, Y.; Kassel, W. S.; Zakharov, L. N.; Rheingold, A. L.; Kemp, R. A. *Inorg. Chem.* **2005**, *44*, 359-364.
(20) Yang, K.-C.; Chang, C.-C.; Yeh, C.-S.; Lee, G.-H.; Peng, S.-M. *Organometallics* **2001**, *20*, 126-137.
(21) Babcock, J. R. Ph. D., University of Chicago, 1998.
(22) Sita, L. R.; Babcock, J. R.; Xi, R. *J. Am. Chem. Soc.* **1996**, *118*, 10912 - 10913.
(23) Wannagat, U.; Kuckertz, H.; Krūger, C.; Pump, J. *Z. Anorg. Allg. Chem.* **1964**, *333*, 54-60.
(24) Castro-Rodriguez, I.; Nakai, H.; Zakharov, L. N.; Rheingold, A. L.; Meyer, K. *Science* **2004**, *305*, 1757-1759.
(25) Baird, M. C.; Wilkinson, G. *J. Chem. Soc. A* **1967**, 865-872.
(26) Coucouvanis, D. *J. Am. Chem. Soc.* **1971**, *93*, 1786-1788.

(27) Fjeldberg, T.; Hope, H.; Lappert, M. F.; Power, P. P.; Thorne, A. J. *J. C. S. Chem. Comm.* **1983**, 639 - 641.
(28) Lappert, M. F.; Power, P. P.; Slade, J. J.; Hedberg, L.; Hedberg, K.; Schomaker, V. *J. Chem. Soc., Chem. Commun.* **1979**, 369 - 370.
(29) Tang, Y.; Zakharov, L. N.; Rheingold, A. L.; Kemp, R. A. *Organometallics* **2004**, *23*, 4788-4791.
(30) Mömming, C. M.; Otten, E.; Kehr, G.; Fröhlich, R.; Grimme, S.; Stephan, D. W.; Erker, G. *Angew. Chem. Int. Ed.* **2009**, *48*, 6643-6646.
(31) Panda, T. K.; Gamer, M. T.; Roesky, P. W. *Inorg. Chim. Acta* **2006**, *359*, 4765-4768.
(32) Roesky, P. W. *Inorg. Chem.* **2006**, *45*, 798-802.
(33) Dickie, D. A.; Parkes, M. V.; Kemp, R. A. *Angew. Chem. Int. Ed.* **2008**, *47*, 9955-9957.
(34) Nöth, H.; Meinel, L. *Z. Anorg. Allg. Chem.* **1967**, *349*, 225-240.
(35) Ellermann, J.; Wend, W. *J. Organomet. Chem.* **1985**, *281*, C29-C32.
(36) Allen, C. F. H.; Bell, A. *Synth. Coll. Vol. III* **1953**, 415-416.
(37) Degerbeck, F.; Grehn, L.; Ragnarsson, U. *Acta Chem. Scand.* **1993**, *47*, 896-898.
(38) Hajra, S.; Bhowmick, M.; Maji, B.; Sinha, D. *J. Org. Chem.* **2007**, *72*, 4872-4876.
(39) Westerhauser, M.; Greul, J.; Hausen, H.-D.; Schwarz, W. *Z. Anorg. Allg. Chem.* **1996**, *622*, 1295 - 1305.
(40) Wrackermeyer, B.; Pedall, A.; Weidinger, J. *Z. Naturforsch.* **2001**, *56b*, 1009 - 1014.

DISTRIBUTION

1	MS0887	Duane B. Dimos	1800
5	MS1349	Richard A. Kemp	1815
1	MS1349	William F. Hammetter	1815
1	MS1349	James E. Miller	1815
1	MS1349	Constantine A. Stewart	1815
1	MS0899	Technical Library	9536 (electronic copy)
1	MS0123	D. Chavez, LDRD Office	1011